

Medius Analysis and Comparison Results for First-Order Finite Element Methods in Linear Elasticity*

C. Carstensen[†] M. Schedensack[‡]

Abstract

This paper enfold a medius analysis for first-order nonconforming finite element methods (FEMs) in linear elasticity named after Crouzeix-Raviart and Kouhia-Stenberg, which are robust with respect to the incompressible limit as the Lamé parameter λ tends to infinity. The new result is a best-approximation error estimate for the stress error in L^2 up to data-oscillation terms. Even for very coarse shape-regular triangulations, two comparison results assert that the errors of the nonconforming FEM are equivalent to that of the conforming first-order FEM. The explicit role of the parameter λ in those equivalence constants leads to an advertisement of the robust and quasi-optimal Kouhia-Stenberg FEM in particular for non-convex polygons. The proofs are based on conforming companions, a new discrete Helmholtz decomposition, and a new discrete-plus-continuous Korn inequality for Kouhia-Stenberg finite element functions. Numerical evidence strongly supports the robustness of the nonconforming FEMs with respect to the incompressibility locking and with respect to singularities and underlines that the dependence of the equivalence constants on λ in the comparison of conforming and nonconforming FEMs cannot be improved. This work therefore advertises the Kouhia-Stenberg FEM as a first-order robust discretisation in linear elasticity in the presence of Neumann boundary conditions.

keywords. linear elasticity, nonconforming finite elements, Kohia-Stenberg, comparison, locking, discrete Korn inequality, Stokes equations

*To appear in IMA J. Numer. Anal.

[†]Institut für Mathematik, Humboldt-Universität zu Berlin, Unter den Linden 6, D-10099 Berlin, Germany; Department of Computational Science and Engineering, Yonsei University, Seoul, Korea

[‡]Institut für Mathematik, Humboldt-Universität zu Berlin, Unter den Linden 6, D-10099 Berlin, Germany

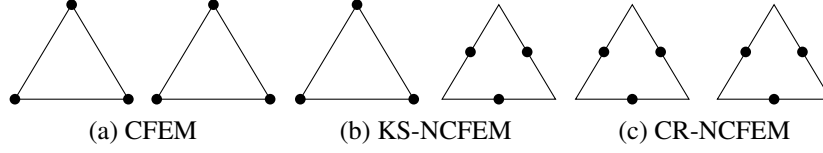


Figure 1.1: Three first-order FEMs for linear elasticity.

AMS subject classifications. 65N15, 65N30, 76M10

1 Introduction

The textbook a priori error analysis of nonconforming finite element methods considers an inconsistency term with the normal derivative of the exact solution along edges and so requires $H^{3/2+\varepsilon}$ regularity of the exact solution for some positive ε . This regularity request fails to hold for certain mixed boundary value problems in linear elasticity and leaves the impression that nonconforming finite element methods (FEMs) may be more sensitive for “near singularities” than conforming FEM [Bra07, p.111 and the web supplement]. The medius analysis of [Gud10, CPS12] does not rely on elliptic regularity at all and proves quasi optimality for the linear elastic model problem of this paper in the sense that the total error is dominated by the approximation error. The medius analysis extends to non-constant coefficients λ and μ and higher space dimensions, while the more involved precise analysis of the singular functions in case of non-convex polygons appears to be limited to the simple linear elastic model problem at hand.

For a polygonal, bounded Lipschitz domain $\Omega \subset \mathbb{R}^2$ with closed Dirichlet boundary Γ_D of positive length and (relatively open) Neumann boundary $\Gamma_N := \partial\Omega \setminus \Gamma_D$ with outer unit normal \mathbf{v} , the strong formulation of the Navier-Lamé equations for volume forces $f \in L^2(\Omega; \mathbb{R}^2)$ and applied tractions $g \in L^2(\Gamma_N; \mathbb{R}^2)$ and homogeneous boundary conditions reads (in compact notation)

$$\begin{aligned} \operatorname{div} \mathbb{C}\varepsilon(u) &= f && \text{in } \Omega, \\ u &= 0 && \text{on } \Gamma_D, \\ \mathbb{C}\varepsilon(u)\mathbf{v} &= g && \text{on } \Gamma_N. \end{aligned}$$

The fourth-order elasticity tensor acts as $\mathbb{C}A := 2\mu A + \lambda \operatorname{tr}(A)1_{2 \times 2}$ for positive Lamé parameters μ and λ and for any general input variable $A \in \mathbb{R}^{2 \times 2}$ and the linear Green strain is $\varepsilon(u) := (Du + Du^\top)/2$.

The conforming first-order finite element method of Figure 1.1a (also named after Courant (CFEM)) converges, but suffers from the locking in the incompress-

ible limit as $\lambda \rightarrow \infty$ [Bra07, BS08, Fal08]. This means for large values of λ that the L^2 error of the stresses shows the expected convergence rate for a very large number of degrees of freedom only. To overcome this phenomenon, finite element spaces should have good approximation properties for nearly incompressible materials. One possibility is the choice of a higher polynomial degree of the ansatz space (≥ 4) or the use of mixed methods. However, the lowest-order conforming mixed method of Arnold and Winther [AW02] still has 30 degrees of freedom per triangle. An alternative approach are the first-order nonconforming methods of Crouzeix and Raviart [BS92] or of Kouhia and Stenberg [KS95], which do not show such a locking phenomenon and are therefore of great interest. This paper enfoldes a medius error analysis for the nonconforming FEM of Kouhia and Stenberg (KS-NCFEM) of Figure 1.1b in the sense that mathematical arguments from an a posteriori error analysis lead to a priori error estimates. The notion of medius analysis was introduced in [Gud10] and leads to results, which rely on no extra regularity of the weak solution and hold for arbitrarily coarse meshes with certain minimal conditions (a)–(d) of Subsection 2.3. In this point, the error analysis of this paper is a refinement of the error analysis in [KS95]. The main result of this analysis is the best-approximation property of the discrete stress $\sigma_{\text{KS}} := \mathbb{C}\varepsilon_{\text{NC}}(u_{\text{KS}})$ (ε_{NC} or D_{NC} are the piecewise analogues of ε or D) with respect to the exact stress $\sigma := \mathbb{C}\varepsilon(u)$ for the exact and discrete solutions $u \in H^1(\Omega; \mathbb{R}^2)$ and $u_{\text{KS}} \in \text{KS}(\mathcal{T})$; that is

$$\begin{aligned} & \|\sigma - \sigma_{\text{KS}}\|_{L^2(\Omega)} \\ & \lesssim \min_{v_{\text{KS}} \in \text{KS}(\mathcal{T})} \|\sigma - \mathbb{C}\varepsilon_{\text{NC}}(v_{\text{KS}})\|_{L^2(\Omega)} + \text{osc}(f_2, \mathcal{T}) + \text{osc}(g_2, \mathcal{E}(\Gamma_N)). \end{aligned}$$

The definitions of the data-oscillations $\text{osc}(f_2, \mathcal{T})$ and $\text{osc}(g_2, \mathcal{E}(\Gamma_N))$ and the precise definition of the Kouhia-Stenberg FEM space $\text{KS}(\mathcal{T})$ follow in Section 2. The notation $A \lesssim B$ abbreviates an inequality $A \leq CB$ with some mesh-size and λ -independent generic constant $0 < C < \infty$. The constant may depend on the constant $\alpha > 0$ in the conditions (a)–(d) of Subsection 2.3 and on μ . Since the multiplicative constant (hidden behind \lesssim) does not depend on λ , the aforementioned error estimate also holds in the incompressible limit $\lambda \rightarrow \infty$. In other words, the quasi optimal convergence follows for the KS-NCFEM in the Stokes problem as well.

The proof relies on a new discrete Helmholtz decomposition (Theorem 3.1), a new discrete-plus-continuous Korn inequality (Theorem 4.1) and the conforming cubic companion of the nonconforming discrete solution from Lemma 3.3. This conforming companion $J_3 v_{\text{CR}}$ fulfils for all Crouzeix-Raviart functions v_{CR} the

integral mean properties

$$\int_T (v_{\text{CR}} - J_3 v_{\text{CR}}) dx = 0 \quad \text{and} \quad \int_T D_{\text{NC}}(v_{\text{CR}} - J_3 v_{\text{CR}}) dx = 0 \quad \text{for all } T \in \mathcal{T}$$

and some stability and approximation properties.

The nonconforming FEM of Crouzeix and Raviart (CR-NCFEM) [BS92] of Figure 1.1c only allows a discretisation of the pure Dirichlet problem $\Gamma_D = \partial\Omega$, in which the (non-physical) stress $\tilde{\sigma} := \tilde{\mathbb{C}}Du := \mu Du + (\lambda + \mu) \operatorname{div}(u) \mathbf{1}_{2 \times 2}$ appears with its approximation $\tilde{\sigma}_{\text{CR}} := \tilde{\mathbb{C}}D_{\text{NC}}u_{\text{CR}}$ in the Crouzeix-Raviart FEM. The best-approximation result of this paper reads

$$\|\sigma - \mathbb{C}\varepsilon_{\text{NC}}(u_{\text{CR}})\|_{L^2(\Omega)} \lesssim \|\tilde{\sigma} - \tilde{\sigma}_{\text{CR}}\|_{L^2(\Omega)} \lesssim \|\tilde{\sigma} - \Pi_0 \tilde{\sigma}\|_{L^2(\Omega)} + \operatorname{osc}(f, \mathcal{T}).$$

Recent comparison results [Bra09, CPS12] lead to equivalences of approximation classes for the Poisson model problem. The best-approximation results and further analysis of this paper lead to comparison results between the three considered FEMs of Figure 1.1 with explicit dependence on the Lamé parameter λ in the equivalence constants. For the conforming discrete solution u_{C} and the discrete stress $\sigma_{\text{C}} := \mathbb{C}\varepsilon(u_{\text{C}})$, the comparison between KS-NCFEM and CFEM reads

$$\begin{aligned} \lambda^{-1} \|\sigma - \sigma_{\text{C}}\|_{L^2(\Omega)} &\lesssim \|\sigma - \sigma_{\text{KS}}\|_{L^2(\Omega)} \\ &\lesssim \|\sigma - \sigma_{\text{C}}\|_{L^2(\Omega)} + \operatorname{osc}(f_2, \mathcal{T}) + \operatorname{osc}(g_2, \mathcal{E}(\Gamma_N)). \end{aligned} \quad (1.1)$$

A detailed investigation of the gap in the dependence on λ , which is in fact sharp, is included in Section 6. For the pure Dirichlet problem $\Gamma_D = \partial\Omega$ the solutions of CR-NCFEM and KS-NCFEM (with $\tilde{\sigma}_{\text{KS}} := \tilde{\mathbb{C}}D_{\text{NC}}u_{\text{KS}}$) exist and can be compared by

$$\begin{aligned} \|\sigma - \sigma_{\text{CR}}\|_{L^2(\Omega)} &\lesssim \|\sigma - \sigma_{\text{KS}}\|_{L^2(\Omega)} + \operatorname{osc}(f, \mathcal{T}) \quad \text{and} \\ \|\tilde{\sigma} - \tilde{\sigma}_{\text{KS}}\|_{L^2(\Omega)} &\lesssim \|\tilde{\sigma} - \tilde{\sigma}_{\text{CR}}\|_{L^2(\Omega)} + \operatorname{osc}(f_2, \mathcal{T}). \end{aligned}$$

The paper focuses on the 2 dimensional case; the generalisation to higher dimensions is straight forward for CR-NCFEM and CFEM. The generalisation of KS-NCFEM to 3D applies two nonconforming and one conforming FEM to the three components or two conforming and one nonconforming; the mathematical justification will be established in the near future [CH].

Within the scope of low-order methods, despite the equivalence results of this paper, the explicit dependence on the Lamé parameter λ strongly suggests the usage of nonconforming discretisations for nearly incompressible materials. If Neumann boundary conditions are present, this advertises the usage of KS-NCFEM

which, therefore, is apparently far too underrated in the engineering community despite striking numerical examples in [KS95, CF01a]. It may appear strange to employ some scheme which depends on the choice of the coordinate system, but (in the presence of Neumann boundary conditions) the KS-NCFEM is the only known robustly quasi-optimal first-order scheme.

The outline of this paper is as follows. Section 2 introduces the precise notation and states the main results, which imply the error estimates of this introduction. Section 3 presents some preliminary results which include the definition of the conforming companion and the new discrete Helmholtz decomposition. Sections 4–5 prove the main results including the new discrete-plus-continuous Korn inequality. Section 6 concludes the paper with numerical illustrations and provides striking numerical evidence for the equivalence of the three first-order methods and the claimed dependence on the equivalence constant as $\lambda \rightarrow \infty$.

Throughout this paper, standard notation on Lebesgue and Sobolev spaces and their norms is employed and further notation can be found in the following table for convenient reading.

$A \lesssim B$	$A \leq CB$ with a mesh-size independent constant C
$v_k, v(k)$	the k -th component of $v \in \mathbb{R}^2$
$A(k, j)$	the component kj of $A \in \mathbb{R}^{2 \times 2}$
$A(k)$	the k -th row $(A(k, 1), A(k, 2))$ of $A \in \mathbb{R}^{2 \times 2}$
$a \cdot b$	$= \sum_{j=1}^2 a(j)b(j)$ for $a, b \in \mathbb{R}^2$
$A : B$	$= \sum_{j,k=1,2} A(j, k)B(j, k)$ for $A, B \in \mathbb{R}^{2 \times 2}$
$1_{2 \times 2}$	unit matrix in $\mathbb{R}^{2 \times 2}$
\mathbb{S}	set of symmetric matrices; $\mathbb{S} := \{A \in \mathbb{R}^{2 \times 2} \mid A = A^\top\}$
$\varepsilon(u)$	Green strain $(Du + (Du)^\top)/2$
\mathbb{C}	elasticity tensor; $\mathbb{C}A = 2\mu A + \lambda \operatorname{tr}(A)1_{2 \times 2}$ for $A \in \mathbb{R}^{2 \times 2}$
$\tilde{\mathbb{C}}$	modified elasticity tensor; $\tilde{\mathbb{C}}A = \mu A + (\mu + \lambda) \operatorname{tr}(A)1_{2 \times 2}$ for $A \in \mathbb{R}^{2 \times 2}$
$C_D(\Omega)$ (resp. $C_N(\Omega)$)	space of continuous functions with homogeneous boundary conditions on Γ_D (resp. Γ_N)
V	$V := \{v \in H^1(\Omega; \mathbb{R}^2) \mid v _{\Gamma_D} = 0\}$
$Dv, \nabla w, \operatorname{div} v$	derivative (of a vector valued function $v \in V$), gradient of a scalar-valued function $w \in H^1(\Omega)$, divergence of v
Curl	$\operatorname{Curl} v = (\partial v / \partial x_2, -\partial v / \partial x_1) \in L^2(\Omega; \mathbb{R}^2)$ for $v \in H^1(\Omega)$, $\operatorname{Curl} w = (\operatorname{Curl} w(1); \operatorname{Curl} w(2)) \in L^2(\Omega; \mathbb{R}^{2 \times 2})$ for $w \in V$

$\mathcal{T}, \mathcal{N}, \mathcal{E}$	shape-regular triangulation with set of vertices \mathcal{N} and set of edges \mathcal{E} , cf. Subsect. 2.2
$\mathcal{N}(\omega)$	set of vertices in ω , $\mathcal{N}(\omega) := \mathcal{N} \cap \omega$
$\mathcal{E}(\omega)$	$= \{E \in \mathcal{E} \mid E \subseteq \bar{\omega}, E \not\subseteq \partial\omega\}$
$ T , E $	area of a triangle T , length of an edge E
$P_k(\mathcal{T}; \mathbb{R}^m)$	set of piecewise polynomials of degree $\leq k$, Subsect. 2.2
Π_0	$\Pi_0 : L^2(\Omega; \mathbb{R}^m) \rightarrow P_0(\mathcal{T}; \mathbb{R}^m)$, L^2 projection on piecewise constants, Subsect. 2.2
$\Pi_{\mathcal{E}}$	L^2 projection onto \mathcal{E} -piecewise constants, Subsect. 2.2
$h_{\mathcal{T}}$	piecewise constant mesh-size, $h_{\mathcal{T}} _T := \text{diam}(T)$ for all T
$[v]_E$	jump along an edge E , Subsect. 2.2
$\text{osc}(f, T), \text{osc}(f, \mathcal{T})$	oscillations of f , $\text{osc}(f, T) := \ h_{\mathcal{T}}(f - \Pi_0 f)\ _{L^2(T)}$, $\text{osc}(f, \mathcal{T}) := \ h_{\mathcal{T}}(f - \Pi_0 f)\ _{L^2(\Omega)}$
$\text{osc}(g, \mathcal{E}(\Gamma_N))$	edge oscillations, Subsect. 2.2
$D_{\text{NC}}, \nabla_{\text{NC}}, \text{div}_{\text{NC}}, \text{Curl}_{\text{NC}}$	piecewise versions of $D, \nabla, \text{div}, \text{Curl}$
$V_{\text{C}}(\mathcal{T})$	conforming finite element space, cf. Subsect. 2.3
$\text{CR}_D^1(\mathcal{T})$	nonconforming Crouzeix-Raviart space, cf. Subsect. 2.3
$V_{\text{CR}}(\mathcal{T})$	$V_{\text{CR}}(\mathcal{T}) := \text{CR}_D^1(\mathcal{T}) \times \text{CR}_D^1(\mathcal{T})$
$\text{KS}(\mathcal{T})$	finite element space of KS-NCFEM; $\text{KS}(\mathcal{T}) = (P_1(\mathcal{T}) \cap C_D(\Omega)) \times \text{CR}_D^1(\mathcal{T})$, cf. Subsect. 2.3
$\text{KS}^*(\mathcal{T})$	$\text{KS}^*(\mathcal{T}) = \text{CR}_N^1(\mathcal{T}) \times (P_1(\mathcal{T}) \cap C_N(\Omega))$, cf. Sect. 3
$I_{\text{NC}} : V \rightarrow V_{\text{CR}}(\mathcal{T})$	nonconforming interpolation operator with $(I_{\text{NC}} v)(\text{mid}(E)) = \int_E v ds$ for all $E \in \mathcal{E} \setminus \mathcal{E}(\Gamma_D)$
$(\bullet, \bullet)_{\mathbb{C}^{-1}}$	$(\sigma, \tau)_{\mathbb{C}^{-1}} := \int_{\Omega} \sigma : \mathbb{C}^{-1} \tau dx$ for $\sigma, \tau \in L^2(\Omega; \mathbb{S})$

2 Notation and Main Results

This section defines the linear elastic model problem, all the considered FEMs, and states the main results.

2.1 Linear Elasticity

Recall that the elastic body occupies the bounded Lipschitz domain Ω with boundary $\partial\Omega = \Gamma_D \cup \Gamma_N$. We assume that Γ_D consists of finitely many parts which

lie on the outer boundary of Ω (on the unbounded connectivity component of $\mathbb{R}^2 \setminus \Omega$). The weak formulation based on the Green strain, seeks $u \in V := \{v \in H^1(\Omega; \mathbb{R}^2) \mid v|_{\Gamma_D} = 0\}$ such that

$$a(v, u) := \int_{\Omega} \varepsilon(v) : \mathbb{C}\varepsilon(u) dx = \int_{\Omega} f \cdot v dx + \int_{\Gamma_N} g \cdot v ds \quad \text{for all } v \in V. \quad (2.1)$$

For the pure Dirichlet problem, i.e., $\Gamma_D = \partial\Omega$, an integration by parts and the commutation of the derivatives for $C_0^\infty(\Omega; \mathbb{R}^2)$ functions shows that

$$\int_{\Omega} \varepsilon(\bullet) : \mathbb{C}\varepsilon(\bullet) dx = \int_{\Omega} D\bullet : \tilde{\mathbb{C}}D\bullet dx$$

on $V \times C_0^\infty(\Omega; \mathbb{R}^2)$. The denseness of $C_0^\infty(\Omega; \mathbb{R}^2)$ in V implies that the two bilinear forms are identical on $V \times V$. Thus, for the pure Dirichlet problem, the equivalent weak formulation based on the full gradient seeks $u \in H_0^1(\Omega; \mathbb{R}^2)$ with

$$\int_{\Omega} Dv : \tilde{\mathbb{C}}Dudx = \int_{\Omega} f \cdot v dx \quad \text{for all } v \in H_0^1(\Omega; \mathbb{R}^2). \quad (2.2)$$

Define the energy norm $\|\bullet\| := \sqrt{a(\bullet, \bullet)}$ in V and the scalar product

$$(\sigma, \tau)_{\mathbb{C}^{-1}} := \int_{\Omega} \sigma : \mathbb{C}^{-1}\tau dx \quad \text{for all } \sigma, \tau \in L^2(\Omega; \mathbb{S}).$$

2.2 Triangulations

Let \mathcal{T} denote some shape-regular triangulation of a polygonal bounded Lipschitz domain Ω into triangles, i.e., $\bar{\Omega} = \bigcup \mathcal{T}$ and any two distinct triangles are either disjoint or share exactly one common edge or one vertex. Let \mathcal{E} denote the set of edges of \mathcal{T} and \mathcal{N} the set of vertices. Define for $\omega \subset \mathbb{R}^2$ the sets $\mathcal{N}(\omega) := \mathcal{N} \cap \omega$ and $\mathcal{E}(\omega) := \{E \in \mathcal{E} \mid \text{int}(E) \subset \omega\}$ for the relative interior $\text{int}(E)$ of an edge $E \in \mathcal{E}$. We assume that the boundary edges $\mathcal{E}(\partial\Omega)$ match the boundary conditions in the sense that the boundary conditions change only at nodes $\Gamma_D \cap \bar{\Gamma}_N \subseteq \mathcal{N}$. Let

$$\begin{aligned} P_k(\mathcal{T}; \mathbb{R}^m) &:= \{v_k : \mathcal{T} \rightarrow \mathbb{R}^m \mid \forall j = 1, \dots, m, \text{ the component} \\ &\quad v_k(j) \text{ of } v_k \text{ is a polynomial of total degree } \leq k\}, \\ P_k(\mathcal{T}; \mathbb{R}^m) &:= \{v_k : \Omega \rightarrow \mathbb{R}^m \mid \forall T \in \mathcal{T}, v_k|_T \in P_k(\mathcal{T}; \mathbb{R}^m)\} \end{aligned}$$

denote the set of piecewise polynomials; $\Pi_0 : L^2(\Omega; \mathbb{R}^m) \rightarrow P_0(\mathcal{T}; \mathbb{R}^m)$ denotes the L^2 -projection onto \mathcal{T} -piecewise constant functions or vectors, i.e., $(\Pi_0 f)|_T = \int_T f dx := \int_T f dx / |T|$ for all $T \in \mathcal{T}$ with area $|T|$ and all $f \in L^2(\Omega; \mathbb{R}^m)$. The operator $\Pi_{\mathcal{E}}$ denotes the L^2 projection onto \mathcal{E} -piecewise constant functions or

vectors, i.e., $\Pi_{\mathcal{E}}g|_E = \int_E g ds / |E|$ for all edges $E \in \mathcal{E}$ of length $|E|$. The volume oscillations read

$$\text{osc}(f, T) := \|h_{\mathcal{T}}(f - \Pi_0 f)\|_{L^2(T)} \quad \text{and} \quad \text{osc}(f, \mathcal{T}) := \|h_{\mathcal{T}}(f - \Pi_0 f)\|_{L^2(\Omega)}$$

while the edge oscillations read

$$\text{osc}(g, \mathcal{E}(\Gamma_N)) := \sqrt{\sum_{E \in \mathcal{E}(\Gamma_N)} \|h_T^{1/2}(g - \Pi_{\mathcal{E}}g)\|_{L^2(E)}^2}$$

with the piecewise constant mesh-size $h_{\mathcal{T}} \in P_0(\mathcal{T})$ with $h_{\mathcal{T}}|_T := \text{diam}(T)$ for all $T \in \mathcal{T}$. The jump along an interior edge $E \in \mathcal{E}(\Omega)$ with adjacent triangles T_+ and T_- , i.e., $E = T_+ \cap T_-$, is defined by $[v]_E := v|_{T_+} - v|_{T_-}$. Given the homogeneous Dirichlet boundary conditions, the jump along boundary edges $E \in \mathcal{E}(\Gamma_D)$ reads $[v]_E := v|_{T_+}$ for that triangle $T_+ \in \mathcal{T}$ with $E \subset T_+$.

For piecewise affine functions $v_{\text{NC}} \in P_1(\mathcal{T}; \mathbb{R}^2)$ the \mathcal{T} -piecewise gradient $D_{\text{NC}}v_{\text{NC}}$ with $(D_{\text{NC}}v_{\text{NC}})|_T = D(v_{\text{NC}}|_T)$ for all $T \in \mathcal{T}$ and, accordingly, $\varepsilon_{\text{NC}}(v_{\text{NC}})$ and $\text{div}_{\text{NC}}(v_{\text{NC}})$, exists and $D_{\text{NC}}v_{\text{NC}} \in P_0(\mathcal{T}; \mathbb{R}^{2 \times 2})$ and $\varepsilon_{\text{NC}}(v_{\text{NC}}) \in P_0(\mathcal{T}; \mathbb{S})$ and $\text{div}_{\text{NC}}(v_{\text{NC}}) \in P_0(\mathcal{T})$.

2.3 Discrete Spaces

CFEM. The Courant finite element space reads

$$V_{\text{C}}(\mathcal{T}) := (P_1(\mathcal{T}) \cap C_D(\Omega)) \times (P_1(\mathcal{T}) \cap C_D(\Omega)).$$

The corresponding (unique) Galerkin approximation $u_{\text{C}} \in V_{\text{C}}(\mathcal{T})$ satisfies

$$\int_{\Omega} \varepsilon(v_{\text{C}}) : \mathbb{C}\varepsilon(u_{\text{C}}) dx = \int_{\Omega} f \cdot v_{\text{C}} dx + \int_{\Gamma_N} g \cdot v_{\text{C}} ds \quad \text{for all } v_{\text{C}} \in V_{\text{C}}(\mathcal{T}).$$

CR-NCFEM. Define the P_1 nonconforming space

$$\text{CR}^1(\mathcal{T}) := \{v_{\text{CR}} \in P_1(\mathcal{T}) \mid v_{\text{CR}} \text{ is continuous at midpoints of interior edges}\}.$$

The nonconforming Crouzeix-Raviart space reads

$$\text{CR}_D^1(\mathcal{T}) := \{v_{\text{CR}} \in \text{CR}^1(\mathcal{T}) \mid v_{\text{CR}} \text{ vanishes at midpoints of edges } E \in \mathcal{E}(\Gamma_D)\}.$$

Define for the discretisation of the pure Dirichlet problem $\Gamma_D = \partial\Omega$ of linear elasticity the space

$$V_{\text{CR}}(\mathcal{T}) := \text{CR}_D^1(\mathcal{T}) \times \text{CR}_D^1(\mathcal{T}).$$

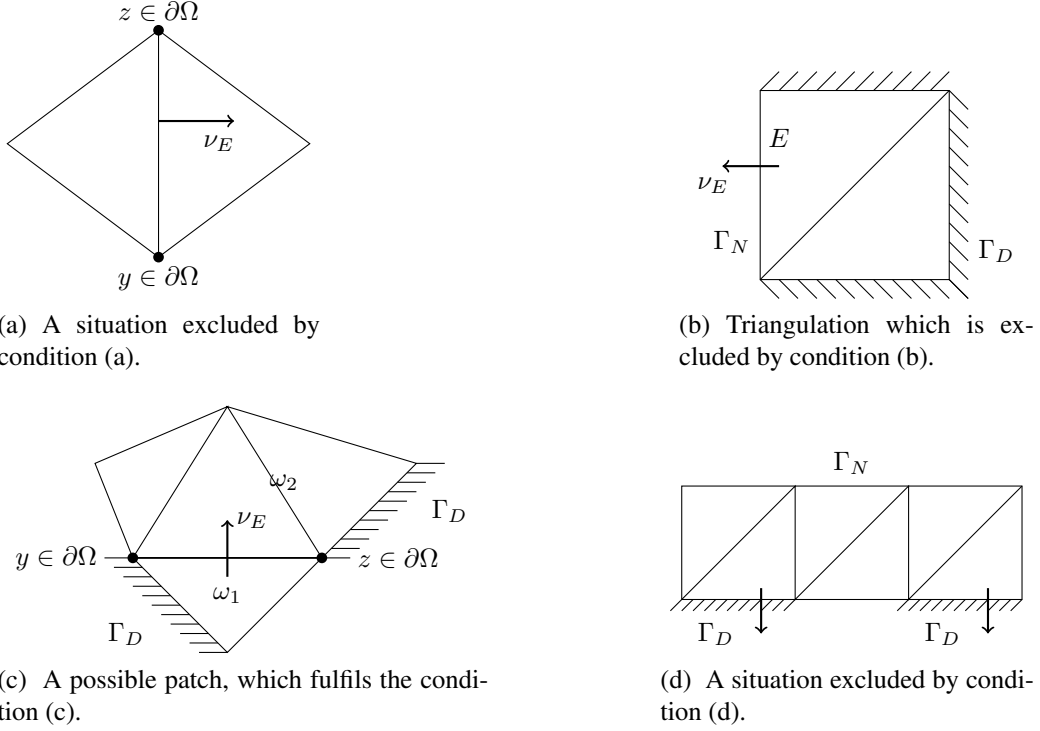


Figure 2.1: Illustrations of the conditions (a)–(d).

Since the kernel of $\epsilon_{\text{NC}} : V_{\text{CR}}(\mathcal{T}) \rightarrow P_0(\mathcal{T}; \mathbb{R}^{2 \times 2})$ is in general not trivial, the weak formulation based on the full gradient is in use for the discretisation and seeks $u_{\text{CR}} \in V_{\text{CR}}(\mathcal{T})$ with

$$\int_{\Omega} D_{\text{NC}} v_{\text{CR}} : \tilde{C} D_{\text{NC}} u_{\text{CR}} dx = \int_{\Omega} f \cdot v_{\text{CR}} dx \quad \text{for all } v_{\text{CR}} \in V_{\text{CR}}(\mathcal{T}). \quad (2.3)$$

Here, the piecewise gradient D_{NC} replaces the weak differential operator.

KS-NCFEM. The Kouhia-Stenberg approximation $u_{\text{KS}} \in \text{KS}(\mathcal{T}) := (P_1(\mathcal{T}) \cap C_D(\Omega)) \times \text{CR}_D^1(\mathcal{T})$ satisfies

$$\int_{\Omega} \epsilon_{\text{NC}}(v_{\text{KS}}) : \mathbb{C} \epsilon_{\text{NC}}(u_{\text{KS}}) dx = \int_{\Omega} f \cdot v_{\text{KS}} dx + \int_{\Gamma_N} g \cdot v_{\text{KS}} ds \quad \text{for all } v_{\text{KS}} \in \text{KS}(\mathcal{T}). \quad (2.4)$$

The following conditions (a)–(d) are given for completeness and replace the assumptions on the sufficiently small mesh-size of \mathcal{T} and the assumptions (AD) and (AN) of [KS95]. These conditions are for example fulfilled if at least one vertex of each triangle lies in the interior of the domain. The existence of $\alpha >$

0 which fulfils the conditions (a)–(d) ensures, that the inf-sup condition and a discrete Korn inequality hold.

- (a) For all $E \in \mathcal{E}(\Omega)$ with $\mathcal{N}(E) \subseteq \mathcal{N}(\partial\Omega)$ it holds $|\mathbf{v}_E(2)| \geq \alpha$.
- (b) If $\Gamma_N \neq \emptyset$ it holds $\mathcal{N} \cap \Gamma_N \neq \emptyset$ or there exists at least one $E \in \mathcal{E}(\Gamma_N)$ with $|\mathbf{v}_E(2)| \geq \alpha$.
- (c) In the case that the two vertices of an interior edge $E \in \mathcal{E}(\Omega)$ belong to the boundary, i.e. $\mathcal{N}(E) \subseteq \mathcal{N}(\partial\Omega)$, and $|\mathbf{v}_E(1)| < \alpha$, consider $z \in \mathcal{N}(E)$. For the nodal patch $\omega_z := \text{int}(\bigcup\{T \in \mathcal{T} \mid z \in T\})$ let $\omega_1, \omega_2 \subseteq \omega_z$ denote the two connected sets, which decompose the nodal patch in the upper and lower part (i.e., $\bar{\omega}_1 \cap \bar{\omega}_2 = E$ and $\omega_1 \cup \omega_2 \cup \text{int}(E) = \omega_z$). Then there exist edges $E_k \in \mathcal{E}(\partial\omega_k) \cap \mathcal{E}(\Gamma_D)$ for $k = 1, 2$ with $|\mathbf{v}_{E_k}(1)| > \alpha$ (see Figure 2.1c).
- (d) If the entire Dirichlet boundary is nearly horizontal, i.e., for all $E \in \mathcal{E}(\Gamma_D)$ it holds $|\mathbf{v}_E(1)| < \alpha$, then there exist two adjacent edges on the Dirichlet boundary, i.e., there exist $E, F \in \mathcal{E}(\Gamma_D)$ with $E \neq F$ and $E \cap F \neq \emptyset$.

The generic multiplicative constants hidden in the notation \lesssim are allowed to depend on α . Figure 2.1 illustrates the conditions (a)–(d).

2.4 Main Results

The main results below imply the statements of the introduction in Section 1.

Theorem 2.1 (best-approximation of KS-NCFEM). *The exact and the discrete stress $\boldsymbol{\sigma} = \mathbb{C}\boldsymbol{\varepsilon}(u)$ and $\boldsymbol{\sigma}_{\text{KS}} = \mathbb{C}\boldsymbol{\varepsilon}_{\text{NC}}(u_{\text{KS}})$ for the exact and discrete solutions $u \in V$ and $u_{\text{KS}} \in \text{KS}(\mathcal{T})$ satisfy*

$$\begin{aligned} \|\boldsymbol{\sigma} - \boldsymbol{\sigma}_{\text{KS}}\|_{L^2(\Omega)} \\ \lesssim \min_{v_{\text{KS}} \in \text{KS}(\mathcal{T})} \|\boldsymbol{\sigma} - \mathbb{C}\boldsymbol{\varepsilon}_{\text{NC}}(v_{\text{KS}})\|_{L^2(\Omega)} + \text{osc}(f_2, \mathcal{T}) + \text{osc}(g_2, \mathcal{E}(\Gamma_N)). \end{aligned}$$

Remark 2.2. As one key ingredient for the proof of Theorem 2.1, the error estimate of Theorem 4.4 from Section 4 estimates the stress error of KS-NCFEM by some best-approximation error of the stress and the derivative in the piecewise constant functions plus some data approximation terms.

Theorem 2.3 (best-approximation of CR-NCFEM). *Let $\tilde{\boldsymbol{\sigma}} := \tilde{\mathbb{C}}Du$ for the exact solution $u \in H_0^1(\Omega; \mathbb{R}^2)$. For the pure Dirichlet problem $\Gamma_D = \partial\Omega$ the discrete stress $\tilde{\boldsymbol{\sigma}}_{\text{CR}} := \tilde{\mathbb{C}}D_{\text{NC}}u_{\text{CR}}$ for the discrete solution $u_{\text{CR}} \in V_{\text{CR}}(\mathcal{T})$ of (2.3) satisfies*

$$\|\tilde{\boldsymbol{\sigma}} - \tilde{\boldsymbol{\sigma}}_{\text{CR}}\|_{L^2(\Omega)} \lesssim \|\tilde{\boldsymbol{\sigma}} - \Pi_0\tilde{\boldsymbol{\sigma}}\|_{L^2(\Omega)} + \text{osc}(f, \mathcal{T}).$$

Theorem 2.4 (comparison of CFEM, CR-NCFEM and KS-NCFEM). *The exact stress $\boldsymbol{\sigma} = \mathbb{C}\boldsymbol{\varepsilon}(u)$ and the discrete stresses $\boldsymbol{\sigma}_C = \mathbb{C}\boldsymbol{\varepsilon}(u_C)$ and $\boldsymbol{\sigma}_{KS} = \mathbb{C}\boldsymbol{\varepsilon}_{NC}(u_{KS})$ satisfy*

$$\begin{aligned} \lambda^{-1} \|\boldsymbol{\sigma} - \boldsymbol{\sigma}_C\|_{L^2(\Omega)} &\lesssim \|\boldsymbol{\sigma} - \boldsymbol{\sigma}_{KS}\|_{L^2(\Omega)} \\ &\lesssim \|\boldsymbol{\sigma} - \boldsymbol{\sigma}_C\|_{L^2(\Omega)} + \text{osc}(f_2, \mathcal{T}) + \text{osc}(g_2, \mathcal{E}(\Gamma_N)). \end{aligned}$$

For the pure Dirichlet problem $\Gamma_D = \partial\Omega$ the discrete stress $\boldsymbol{\sigma}_{CR} = \mathbb{C}\boldsymbol{\varepsilon}_{NC}(u_{CR})$ satisfies

$$\|\boldsymbol{\sigma} - \boldsymbol{\sigma}_{CR}\|_{L^2(\Omega)} \lesssim \|\boldsymbol{\sigma} - \boldsymbol{\sigma}_{KS}\|_{L^2(\Omega)} + \text{osc}(f, \mathcal{T}).$$

In addition, the stress error of KS-NCFEM is comparable with the error of the non-symmetric approximation $\tilde{\boldsymbol{\sigma}} := \tilde{\mathbb{C}}Du$ from (2.2) through

$$\|\boldsymbol{\sigma} - \boldsymbol{\sigma}_{KS}\|_{L^2(\Omega)} \lesssim \|\tilde{\boldsymbol{\sigma}} - \tilde{\boldsymbol{\sigma}}_{CR}\|_{L^2(\Omega)} + \text{osc}(f_2, \mathcal{T}).$$

3 Preliminary Results

The following discrete Helmholtz decomposition and some properties of a conforming companion are required below; cf. [FM90] for a first decomposition of this type. To this end, define

$$\begin{aligned} \text{CR}^*(\mathcal{T}) &:= \{v_{CR} \in \text{CR}(\mathcal{T}) \mid v_{CR}(\text{mid}(E_1)) = v_{CR}(\text{mid}(E_2)) \\ &\quad \text{for } E_1, E_2 \text{ edges of the same connectivity component of } \Gamma_N\}, \\ V_C^*(\mathcal{T}) &:= \{v_C \in P_1(\mathcal{T}) \cap H^1(\Omega) \mid v_C \text{ is constant along} \\ &\quad \text{each connectivity component of } \Gamma_N\}. \end{aligned}$$

Recall that the boundary conditions match the triangulation \mathcal{T} of the possibly multiply connected planar Lipschitz domain Ω with $\Gamma_D \subseteq \Gamma_0$ for the outer boundary Γ_0 of Ω (Γ_0 is defined as the boundary of the unbounded connectivity component of $\mathbb{R}^2 \setminus \Omega$).

Theorem 3.1 (discrete Helmholtz decomposition). *Let $\text{KS}^*(\mathcal{T}) := \text{CR}^*(\mathcal{T}) \times V_C^*(\mathcal{T})$. Then it holds*

$$P_0(\mathcal{T}; \mathbb{S}) = \mathbb{C}\boldsymbol{\varepsilon}_{NC}(\text{KS}(\mathcal{T})) \oplus (\text{Curl}_{NC}(\text{KS}^*(\mathcal{T})) \cap P_0(\mathcal{T}; \mathbb{S}))$$

and the sum is orthogonal with respect to the scalar product $(\bullet, \bullet)_{\mathbb{C}^{-1}} := \int_{\Omega} \bullet : \mathbb{C}^{-1} \bullet \, dx$.

Remark 3.2. For any $v_{KS}^* \in \text{KS}^*(\mathcal{T})$, the assertion $\text{Curl}_{NC} v_{KS}^* \in P_0(\mathcal{T}; \mathbb{S})$ is equivalent to $\text{div}_{NC} v_{KS}^* = 0$.

Proof of Theorem 3.1. For $\alpha_{\text{KS}} \in \text{KS}(\mathcal{T})$ and $\beta_{\text{KS}^*} \in \text{KS}^*(\mathcal{T})$ with $\text{Curl}_{\text{NC}}(\beta_{\text{KS}^*}) \in P_0(\mathcal{T}; \mathbb{S})$ let $\alpha_{\text{C}} \in P_1(\mathcal{T}) \cap C_D(\Omega)$, $\alpha_{\text{CR}} \in \text{CR}_D^1(\mathcal{T})$, $\beta_{\text{CR}} \in \text{CR}^*(\mathcal{T})$ and $\beta_{\text{C}} \in V_{\text{C}}^*(\mathcal{T})$ with $\alpha_{\text{KS}} = (\alpha_{\text{C}}, \alpha_{\text{CR}})$ and $\beta_{\text{KS}^*} = (\beta_{\text{CR}}, \beta_{\text{C}})$. Then α_{KS} and β_{KS^*} satisfy

$$\begin{aligned} (\mathbb{C}\varepsilon(\alpha_{\text{KS}}), \text{Curl}_{\text{NC}} \beta_{\text{KS}^*})_{\mathbb{C}^{-1}} &= \int_{\Omega} \varepsilon_{\text{NC}}(\alpha_{\text{KS}}) : \text{Curl}_{\text{NC}} \beta_{\text{KS}^*} dx \\ &= \int_{\Omega} D_{\text{NC}}(\alpha_{\text{KS}}) : \text{Curl}_{\text{NC}} \beta_{\text{KS}^*} dx \\ &= \int_{\Omega} (\nabla \alpha_{\text{C}} \cdot \text{Curl}_{\text{NC}} \beta_{\text{CR}} + \nabla_{\text{NC}} \alpha_{\text{CR}} \cdot \text{Curl} \beta_{\text{C}}) dx. \end{aligned}$$

This and the L^2 orthogonalities

$$\begin{aligned} \nabla(P_1(\mathcal{T}) \cap C_D(\Omega)) \perp_{L^2} \text{Curl}_{\text{NC}}(\text{CR}^*(\mathcal{T})), \\ \nabla_{\text{NC}} \text{CR}_D^1(\mathcal{T}) \perp_{L^2} \text{Curl}(V_{\text{C}}^*(\mathcal{T})) \end{aligned} \quad (3.1)$$

imply the orthogonality (with respect to the scalar product $(\bullet, \bullet)_{\mathbb{C}^{-1}}$)

$$\mathbb{C}\varepsilon_{\text{NC}}(\text{KS}(\mathcal{T})) \perp (\text{Curl}_{\text{NC}}(\text{KS}^*(\mathcal{T})) \cap P_0(\mathcal{T}; \mathbb{S})).$$

Given $\sigma_h \in P_0(\mathcal{T}; \mathbb{S})$, let $\alpha_{\text{KS}} \in \text{KS}(\mathcal{T})$ solve

$$\int_{\Omega} \varepsilon_{\text{NC}}(v_{\text{KS}}) : \mathbb{C}\varepsilon_{\text{NC}}(\alpha_{\text{KS}}) dx = \int_{\Omega} \varepsilon_{\text{NC}}(v_{\text{KS}}) : \sigma_h dx \quad \text{for all } v_{\text{KS}} \in \text{KS}(\mathcal{T}).$$

The j -th row $\tau_h(j) := (\tau_h(j, 1), \tau_h(j, 2)) \in P_0(\mathcal{T}; \mathbb{R}^2)$ of $\tau_h := \sigma_h - \mathbb{C}\varepsilon_{\text{NC}}(\alpha_{\text{KS}}) \in P_0(\mathcal{T}; \mathbb{S})$ is piecewise constant for $j = 1, 2$. The discrete Helmholtz decomposition for Crouzeix-Raviart and conforming P_1 functions [AF89] remains true for mixed boundary conditions and interchanged discrete spaces as

$$\begin{aligned} P_0(\mathcal{T}; \mathbb{R}^2) &= \nabla_{\text{NC}} \text{CR}_D^1(\mathcal{T}) \oplus \text{Curl} V_{\text{C}}^*(\mathcal{T}); \\ P_0(\mathcal{T}; \mathbb{R}^2) &= \nabla(P_1(\mathcal{T}) \cap C_D(\Omega)) \oplus \text{Curl}_{\text{NC}} \text{CR}^*(\mathcal{T}). \end{aligned}$$

(This can be proved, e.g., by the orthogonalities (3.1) and a dimension argument). This guarantees the existence of $p_{\text{C}} \in P_1(\mathcal{T}) \cap C_D(\Omega)$, $p_{\text{CR}} \in \text{CR}^*(\mathcal{T})$, $q_{\text{CR}} \in \text{CR}_D^1(\mathcal{T})$ and $q_{\text{C}} \in V_{\text{C}}^*(\mathcal{T})$ with

$$\tau_h(1) = \nabla p_{\text{C}} + \text{Curl}_{\text{NC}} p_{\text{CR}} \quad \text{and} \quad \tau_h(2) = \nabla_{\text{NC}} q_{\text{CR}} + \text{Curl} q_{\text{C}}.$$

(Here, ∇p_{C} , $\text{Curl}_{\text{NC}} p_{\text{CR}}$, $\nabla_{\text{NC}} q_{\text{CR}}$, and $\text{Curl} q_{\text{C}}$ are understood as row vectors.) Since τ_h is orthogonal to $\mathbb{C}\varepsilon_{\text{NC}}(\text{KS}(\mathcal{T}))$ with respect to $(\bullet, \bullet)_{\mathbb{C}^{-1}}$ and since $\tau_h \in P_0(\mathcal{T}; \mathbb{S})$, the functions $v_{\text{C}} \in P_1(\mathcal{T}) \cap C_D(\Omega)$ and $v_{\text{CR}} \in \text{CR}_D^1(\mathcal{T})$ satisfy

$$\int_{\Omega} (\nabla v_{\text{C}}; \nabla_{\text{NC}} v_{\text{CR}}) : (\tau_h(1); \tau_h(2)) dx = \int_{\Omega} \varepsilon_{\text{NC}}(v_{\text{C}}, v_{\text{CR}}) : \tau_h dx = 0.$$

This implies the L^2 orthogonalities

$$\tau_h(1) \perp_{L^2} \nabla(P_1(\mathcal{T}) \cap C_D(\Omega)) \quad \text{and} \quad \tau_h(2) \perp_{L^2} \nabla_{\text{NC}} \text{CR}_D^1(\mathcal{T}).$$

This and the orthogonalities (3.1) lead to

$$\|\nabla p_C\|_{L^2(\Omega)}^2 = \int_{\Omega} \nabla p_C \cdot (\nabla p_C - \tau_h(1)) dx = 0.$$

Analogue arguments prove $\|\nabla_{\text{NC}} q_{\text{CR}}\|_{L^2(\Omega)}^2 = 0$. Hence,

$$\tau_h = \text{Curl}_{\text{NC}}(p_{\text{CR}}, q_{\text{CR}}) \in \text{Curl}_{\text{NC}}(\text{KS}^*(\mathcal{T})). \quad \square$$

Lemma 3.3. *There exists an operator $J_3 : \text{CR}_D^1(\mathcal{T}) \rightarrow (P_3(\mathcal{T}) \cap C_D(\Omega))$ with the conservation properties*

$$\int_T (v_{\text{CR}} - J_3 v_{\text{CR}}) dx = 0 \quad \text{for all } T \in \mathcal{T}, \quad (3.2.a)$$

$$\int_E (v_{\text{CR}} - J_3 v_{\text{CR}}) dx = 0 \quad \text{for all } E \in \mathcal{E} \quad (3.2.b)$$

and the approximation and stability properties

$$\begin{aligned} \left\| h_T^{-1} (v_{\text{CR}} - J_3 v_{\text{CR}}) \right\|_{L^2(\Omega)} &\approx \|\nabla_{\text{NC}}(v_{\text{CR}} - J_3 v_{\text{CR}})\|_{L^2(\Omega)} \\ &\approx \min_{\varphi \in H^1(\Omega) \cap C_D(\Omega)} \|\nabla_{\text{NC}}(v_{\text{CR}} - \varphi)\|_{L^2(\Omega)} \\ &\leq \|\nabla_{\text{NC}} v_{\text{CR}}\|_{L^2(\Omega)}. \end{aligned} \quad (3.3)$$

Remark 3.4. The conservation property along edges (3.2.b) and an integration by parts reveal the conservation property of the gradients $\Pi_0 \nabla J_3 = \nabla_{\text{NC}}$ in the sense that

$$\int_T \nabla J_3 v_{\text{CR}} dx = \int_T \nabla_{\text{NC}} v_{\text{CR}} dx \quad \text{for all } T \in \mathcal{T} \text{ and all } v_{\text{CR}} \in \text{CR}_D^1(\mathcal{T}).$$

Proof of Lemma 3.3. The design is based on three successive steps.

Step 1. The operator $J_1 : \text{CR}_D^1(\mathcal{T}) \rightarrow P_1(\mathcal{T}) \cap C_D(\Omega)$ acts on any function $v_{\text{CR}} \in \text{CR}_D^1(\mathcal{T})$ by averaging the function values at each node $z \in \mathcal{N}(\Omega \cup \Gamma_N)$

$$J_1 v_{\text{CR}}(z) = |\mathcal{T}(z)|^{-1} \sum_{T \in \mathcal{T}(z)} v_{\text{CR}}|_T(z) \quad \text{for all } z \in \mathcal{N}(\Omega \cup \Gamma_N) \quad (3.4)$$

with $\mathcal{T}(z) := \{T \in \mathcal{T} \mid z \in T\}$. (This operator is also known as enriching operator in the context of fast solvers [Bre96].) The arguments of [CEHL12, Theorem 5.1] prove the approximation property

$$\begin{aligned} \left\| h_{\mathcal{T}}^{-1}(v_{\text{CR}} - J_1 v_{\text{CR}}) \right\|_{L^2(\Omega)} &\lesssim \sqrt{\sum_{E \in \mathcal{E}(\Omega \cup \Gamma_D)} |E|^{-1} \|[v_{\text{CR}}]_E\|_{L^2(E)}^2} \\ &\lesssim \sqrt{\sum_{E \in \mathcal{E}(\Omega \cup \Gamma_D)} |E| \|\nabla_{\text{NC}} v_{\text{CR}} \cdot \boldsymbol{\tau}_E\|_{L^2(E)}^2} \quad (3.5) \\ &\lesssim \min_{v \in H^1(\Omega) \cap C_D(\Omega)} \|\nabla_{\text{NC}}(v_{\text{CR}} - v)\|_{L^2(\Omega)}. \end{aligned}$$

This and an inverse estimate imply the stability property

$$\|\nabla_{\text{NC}}(v_{\text{CR}} - J_1 v_{\text{CR}})\|_{L^2(\Omega)} \lesssim \min_{v \in H^1(\Omega) \cap C_D(\Omega)} \|\nabla_{\text{NC}}(v_{\text{CR}} - v)\|_{L^2(\Omega)}. \quad (3.6)$$

Step 2. Given any edge $E = \text{conv}\{a, b\} \in \mathcal{E}(\Omega \cup \Gamma_N)$ with nodal P_1 conforming basis functions $\varphi_a, \varphi_b \in P_1(\mathcal{T}) \cap C(\Omega)$ (defined by $\varphi_a(a) = 1$ and $\varphi_a(z) = 0$ for $z \in \mathcal{N} \setminus \{a\}$), the quadratic edge-bubble function

$$\mathfrak{b}_E := 6\varphi_a\varphi_b$$

has the support $\overline{\omega}_E$ and satisfies $\int_E \mathfrak{b}_E ds = 1$. For any function $v_{\text{CR}} \in \text{CR}_D^1(\mathcal{T})$ the operator $J_2 : \text{CR}_D^1(\mathcal{T}) \rightarrow P_2(\mathcal{T}) \cap C_D(\Omega)$ acts as

$$J_2 v_{\text{CR}} := J_1 v_{\text{CR}} + \sum_{E \in \mathcal{E}(\Omega \cup \Gamma_N)} \left(\int_E (v_{\text{CR}} - J_1 v_{\text{CR}}) ds \right) \mathfrak{b}_E.$$

An immediate consequence of this choice is

$$\int_E J_2 v_{\text{CR}} ds = \int_E v_{\text{CR}} ds \quad \text{for all } E \in \mathcal{E}.$$

An integration by parts shows for the vertex $P_E \in \mathcal{N}(T) \setminus E$ opposite to $E \in \mathcal{E}(T)$ in the triangle T the trace identity

$$\begin{aligned} &\int_E (v_{\text{CR}} - J_1 v_{\text{CR}}) ds \\ &= \int_T (v_{\text{CR}} - J_1 v_{\text{CR}}) dx + \frac{1}{2} \int_T (x - P_E) \cdot \nabla_{\text{NC}}(v_{\text{CR}} - J_1 v_{\text{CR}}) dx. \end{aligned}$$

The scaling $\|\mathbf{b}_E\|_{L^2(\Omega)} \lesssim h_T$ shows

$$\begin{aligned} \left\| h_T^{-1} \sum_{E \in \mathcal{E}(T)} \left(\int_E (v_{\text{CR}} - J_1 v_{\text{CR}}) ds \right) \mathbf{b}_E \right\|_{L^2(T)} &\lesssim \sum_{E \in \mathcal{E}(T)} \left| \int_E (v_{\text{CR}} - J_1 v_{\text{CR}}) ds \right| \\ &\lesssim h_T^{-1} \|v_{\text{CR}} - J_1 v_{\text{CR}}\|_{L^2(T)} + \|\nabla_{\text{NC}}(v_{\text{CR}} - J_1 v_{\text{CR}})\|_{L^2(T)}. \end{aligned}$$

This and (3.5)–(3.6) yield

$$\left\| h_T^{-1} (v_{\text{CR}} - J_2 v_{\text{CR}}) \right\|_{L^2(\Omega)} \lesssim \min_{v \in H^1(\Omega) \cap C_D(\Omega)} \|\nabla_{\text{NC}}(v_{\text{CR}} - v)\|_{L^2(\Omega)}. \quad (3.7)$$

The stability property of J_2 follows with an inverse estimate

$$\begin{aligned} \|\nabla_{\text{NC}}(v_{\text{CR}} - J_2 v_{\text{CR}})\|_{L^2(\Omega)} &\lesssim \left\| h_T^{-1} (v_{\text{CR}} - J_2 v_{\text{CR}}) \right\|_{L^2(\Omega)} \\ &\lesssim \min_{v \in H^1(\Omega) \cap C_D(\Omega)} \|\nabla_{\text{NC}}(v_{\text{CR}} - v)\|_{L^2(\Omega)}. \end{aligned} \quad (3.8)$$

Step 3. On any triangle $T = \text{conv}\{a, b, c\}$ with nodal basis functions $\varphi_a, \varphi_b, \varphi_c$, the cubic volume bubble function reads

$$\mathbf{b}_T := 60\varphi_a\varphi_b\varphi_c \in H_0^1(T).$$

and enjoys the scaling $\|\nabla \mathbf{b}_T\|_{L^2(\Omega)} \approx 1$. Define

$$J_3 v_{\text{CR}} := J_2 v_{\text{CR}} + \sum_{T \in \mathcal{T}} \left(\int_T (v_{\text{CR}} - J_2 v_{\text{CR}}) dx \right) \mathbf{b}_T.$$

Then J_3 fulfils the conservation properties (3.2) and

$$\begin{aligned} \left\| \sum_{T \in \mathcal{T}} \left(\int_T (v_{\text{CR}} - J_2 v_{\text{CR}}) dx \right) \nabla \mathbf{b}_T \right\|_{L^2(\Omega)}^2 &\approx \sum_{T \in \mathcal{T}} \left| \int_T (v_{\text{CR}} - J_2 v_{\text{CR}}) dx \right|^2 \\ &\lesssim \left\| h_T^{-1} (v_{\text{CR}} - J_2 v_{\text{CR}}) \right\|_{L^2(\Omega)}^2. \end{aligned}$$

This and (3.7)–(3.8) imply

$$\begin{aligned} &\|D_{\text{NC}}(v_{\text{CR}} - J_3 v_{\text{CR}})\|_{L^2(\Omega)} \\ &\leq \|D_{\text{NC}}(v_{\text{CR}} - J_2 v_{\text{CR}})\|_{L^2(\Omega)} + \left\| \sum_{T \in \mathcal{T}} \left(\int_T (v_{\text{CR}} - J_2 v_{\text{CR}}) dx \right) \nabla \mathbf{b}_T \right\|_{L^2(\Omega)} \\ &\lesssim \min_{v \in H^1(\Omega) \cap C_D(\Omega)} \|\nabla_{\text{NC}}(v_{\text{CR}} - v)\|_{L^2(\Omega)}. \end{aligned}$$

This and some Poincaré inequality lead to (3.3). \square

Lemma 3.5. Any $v_{\text{KS}} \in \text{KS}(\mathcal{T})$ satisfies

$$\begin{aligned} \int_{\Omega} (\Pi_0 \sigma - \sigma_{\text{KS}}) : \varepsilon_{\text{NC}}(v_{\text{KS}}) dx &\lesssim (\|(\sigma - \Pi_0 \sigma)(2)\|_{L^2(\Omega)} + \text{osc}(f_2, \mathcal{T}) \\ &\quad + \text{osc}(g_2, \mathcal{E}(\Gamma_N))) \|\nabla_{\text{NC}} v_{\text{KS}}(2)\|_{L^2(\Omega)}. \end{aligned}$$

Proof. Given any $v_{\text{KS}} \in \text{KS}(\mathcal{T})$ let $v_{\text{KS}} = (v_{\text{C}}, v_{\text{CR}})$ be with $v_{\text{C}} \in P_1(\mathcal{T}) \cap C_D(\Omega)$ and $v_{\text{CR}} \in \text{CR}_D^1(\mathcal{T})$. Lemma 3.3 guarantees the existence of $J_3 v_{\text{CR}} \in P_3(\mathcal{T}) \cap H^1(\Omega) \cap C_D(\Omega)$ with

$$\begin{aligned} \int_T (v_{\text{CR}} - J_3 v_{\text{CR}}) dx = 0 &= \int_T \nabla_{\text{NC}}(v_{\text{CR}} - J_3 v_{\text{CR}}) dx \quad \text{for all } T \in \mathcal{T} \\ \text{and } \|\nabla_{\text{NC}}(v_{\text{CR}} - J_3 v_{\text{CR}})\|_{L^2(\Omega)} &\lesssim \|\nabla_{\text{NC}} v_{\text{CR}}\|_{L^2(\Omega)}. \end{aligned} \quad (3.9)$$

Since $\Pi_0 \sigma$ is piecewise constant, the integral mean property (3.9) implies

$$\begin{aligned} \int_{\Omega} \Pi_0 \sigma : \varepsilon_{\text{NC}}(0, v_{\text{CR}}) dx &= \int_{\Omega} \Pi_0 \sigma : \varepsilon_{\text{NC}}(0, J_3 v_{\text{CR}}) dx \\ &= \int_{\Omega} (\Pi_0 \sigma - \sigma) : D(0, J_3 v_{\text{CR}}) dx + \int_{\Omega} \sigma : \varepsilon(0, J_3 v_{\text{CR}}) dx. \end{aligned}$$

Since σ is the stress of the exact solution and $J_3 v_{\text{CR}} \in H^1(\Omega) \cap C_D(\Omega)$, the Cauchy-Schwarz inequality implies

$$\begin{aligned} &\int_{\Omega} (\Pi_0 \sigma - \sigma) : D(0, J_3 v_{\text{CR}}) dx + \int_{\Omega} \sigma : \varepsilon(0, J_3 v_{\text{CR}}) dx \\ &\leq \|(\sigma - \Pi_0 \sigma)(2)\|_{L^2(\Omega)} \|\nabla J_3 v_{\text{CR}}\|_{L^2(\Omega)} + \int_{\Omega} f_2 J_3 v_{\text{CR}} dx + \int_{\Gamma_N} g_2 J_3 v_{\text{CR}} ds. \end{aligned}$$

The triangle inequality and the stability property (3.9) show

$$\begin{aligned} \|\nabla J_3 v_{\text{CR}}\|_{L^2(\Omega)} &\leq \|\nabla J_3 v_{\text{CR}} - \nabla_{\text{NC}} v_{\text{CR}}\|_{L^2(\Omega)} + \|\nabla_{\text{NC}} v_{\text{CR}}\|_{L^2(\Omega)} \\ &\lesssim \|\nabla_{\text{NC}} v_{\text{CR}}\|_{L^2(\Omega)}. \end{aligned}$$

The combination of the above inequalities yields

$$\begin{aligned} &\int_{\Omega} \Pi_0 \sigma : \varepsilon_{\text{NC}}(0, v_{\text{CR}}) dx \\ &\lesssim \|(\sigma - \Pi_0 \sigma)(2)\|_{L^2(\Omega)} \|\nabla_{\text{NC}} v_{\text{CR}}\|_{L^2(\Omega)} + \int_{\Omega} f_2 J_3 v_{\text{CR}} dx + \int_{\Gamma_N} g_2 J_3 v_{\text{CR}} ds. \end{aligned}$$

Since σ and σ_{KS} are the stresses of the exact and the discrete solution, it follows

$$\begin{aligned} & \int_{\Omega} (\Pi_0 \sigma - \sigma_{\text{KS}}) : \varepsilon_{\text{NC}}(v_{\text{KS}}) dx \\ &= \int_{\Omega} (\Pi_0 \sigma - \sigma_{\text{KS}}) : \varepsilon_{\text{NC}}(0, v_{\text{CR}}) dx \\ &= \int_{\Omega} \Pi_0 \sigma : \varepsilon_{\text{NC}}(0, v_{\text{CR}}) dx - \int_{\Omega} f_2 v_{\text{CR}} dx - \int_{\Gamma_N} g_2 v_{\text{CR}} ds. \end{aligned}$$

The combination of the previous displayed formulas proves

$$\begin{aligned} & \int_{\Omega} (\Pi_0 \sigma - \sigma_{\text{KS}}) : \varepsilon_{\text{NC}}(v_{\text{KS}}) dx \\ & \lesssim \|(\sigma - \Pi_0 \sigma)(2)\|_{L^2(\Omega)} \|\nabla_{\text{NC}} v_{\text{CR}}\|_{L^2(\Omega)} \\ & \quad + \int_{\Omega} f_2 (J_3 v_{\text{CR}} - v_{\text{CR}}) dx + \int_{\Gamma_N} g_2 (J_3 v_{\text{CR}} - v_{\text{CR}}) ds. \end{aligned} \tag{3.10}$$

Since the integral mean of $J_3 v_{\text{CR}} - v_{\text{CR}}$ vanishes on triangles, the trace inequality [BS08, p.282] followed by a Poincaré inequality yields for $E \in \mathcal{E}(\Gamma_N)$ and $T \in \mathcal{T}$ with $E \in \mathcal{E}(T)$

$$\begin{aligned} & \|h_T^{-1/2} (J_3 v_{\text{CR}} - v_{\text{CR}})\|_{L^2(E)} \\ & \lesssim \|h_T^{-1} (J_3 v_{\text{CR}} - v_{\text{CR}})\|_{L^2(T)} + \|\nabla_{\text{NC}} (J_3 v_{\text{CR}} - v_{\text{CR}})\|_{L^2(T)} \\ & \leq \|\nabla_{\text{NC}} (J_3 v_{\text{CR}} - v_{\text{CR}})\|_{L^2(T)}. \end{aligned}$$

Since the integral mean of $J_3 v_{\text{CR}} - v_{\text{CR}}$ vanishes on edges, this leads to

$$\int_E g_2 (J_3 v_{\text{CR}} - v_{\text{CR}}) ds \lesssim \|h_T^{1/2} (g_2 - \Pi_E g_2)\|_{L^2(E)} \|\nabla_{\text{NC}} (J_3 v_{\text{CR}} - v_{\text{CR}})\|_{L^2(T)}.$$

Since the integral mean of $J_3 v_{\text{CR}} - v_{\text{CR}}$ vanishes on triangles, (3.10) implies

$$\begin{aligned} & \int_{\Omega} (\Pi_0 \sigma - \sigma_{\text{KS}}) : \varepsilon_{\text{NC}}(v_{\text{KS}}) dx \\ & \lesssim (\|(\sigma - \Pi_0 \sigma)(2)\|_{L^2(\Omega)} + \text{osc}(f_2, \mathcal{T}) + \text{osc}(g_2, \mathcal{E}(\Gamma_N))) \|\nabla_{\text{NC}} v_{\text{CR}}\|_{L^2(\Omega)}. \end{aligned}$$

This concludes the proof. \square

The nonconforming interpolation operator $I_{\text{NC}} : V \rightarrow V_{\text{CR}}(\mathcal{T})$ is defined by $(I_{\text{NC}} v)(\text{mid}(E)) = \int_E v ds$ for all $E \in \mathcal{E} \setminus \mathcal{E}(\Gamma_D)$ and fulfils the integral mean property $D_{\text{NC}} I_{\text{NC}} = \Pi_0 D$ in the sense that

$$D_{\text{NC}} I_{\text{NC}} v|_T = \int_T Dv dx \quad \text{for all } T \in \mathcal{T} \text{ and all } v \in V. \tag{3.11}$$

Lemma 3.6. Any $\beta_{\text{KS}^*} \in \text{KS}^*(\mathcal{T})$ with $\text{Curl}_{\text{NC}} \beta_{\text{KS}^*} \in P_0(\mathcal{T}; \mathbb{S})$ satisfies

$$\begin{aligned} \int_{\Omega} \varepsilon_{\text{NC}}(I_{\text{NC}}u - u_{\text{KS}}) : \text{Curl}_{\text{NC}} \beta_{\text{KS}^*} dx \\ \lesssim \|(Du - \Pi_0 Du)(1)\|_{L^2(\Omega)} \|\text{Curl}_{\text{NC}} \beta_{\text{KS}^*}(1)\|_{L^2(\Omega)}. \end{aligned}$$

Proof. According to the definition, $\beta_{\text{KS}^*}(1) \in \text{CR}^*(\mathcal{T})$ and $\beta_{\text{KS}^*}(2) \in V_{\mathbb{C}}^*(\mathcal{T})$. The orthogonalities (3.1) and $\text{Curl}_{\text{NC}} \beta_{\text{KS}^*} \in \mathbb{S}$ show, for any $\phi_{\mathbb{C}} \in P_1(\mathcal{T}) \cap C_D(\Omega)$, that

$$\begin{aligned} \int_{\Omega} \varepsilon_{\text{NC}}(I_{\text{NC}}u - u_{\text{KS}}) : \text{Curl}_{\text{NC}} \beta_{\text{KS}^*} dx \\ = \int_{\Omega} (\nabla_{\text{NC}} I_{\text{NC}}u(1) - \nabla \phi_{\mathbb{C}}) \cdot \text{Curl}_{\text{NC}} \beta_{\text{KS}^*}(1) dx. \end{aligned}$$

Since $\phi_{\mathbb{C}} \in P_1(\mathcal{T}) \cap C_D(\Omega)$ is arbitrary, this implies

$$\begin{aligned} \int_{\Omega} \varepsilon_{\text{NC}}(I_{\text{NC}}u - u_{\text{KS}}) : \text{Curl}_{\text{NC}} \beta_{\text{KS}^*} dx \\ \leq \min_{\phi_{\mathbb{C}} \in P_1(\mathcal{T}) \cap C_D(\Omega)} \|\nabla_{\text{NC}} I_{\text{NC}}u(1) - \nabla \phi_{\mathbb{C}}\|_{L^2(\Omega)} \|\text{Curl}_{\text{NC}} \beta_{\text{KS}^*}(1)\|_{L^2(\Omega)}. \end{aligned} \quad (3.12)$$

The integral mean property (3.11) of I_{NC} and [CEHL12, Theorem 5.1] show

$$\begin{aligned} \min_{\phi_{\mathbb{C}} \in P_1(\mathcal{T}) \cap C_D(\Omega)} \|\nabla_{\text{NC}} I_{\text{NC}}u(1) - \nabla \phi_{\mathbb{C}}\|_{L^2(\Omega)} &\leq \|\nabla u(1) - \nabla_{\text{NC}} I_{\text{NC}}u(1)\|_{L^2(\Omega)} \\ &= \|\nabla u(1) - \Pi_0 \nabla u(1)\|_{L^2(\Omega)}. \end{aligned} \quad (3.13)$$

The combination of (3.12)–(3.13) concludes the proof. \square

4 Proof of Theorem 2.1

The main step in the proof of Theorem 2.1 is the error estimate

$$\begin{aligned} \|\sigma - \sigma_{\text{KS}}\|_{L^2(\Omega)} &\lesssim \|\sigma - \Pi_0 \sigma\|_{L^2(\Omega)} + \|(Du - \Pi_0 Du)(1)\|_{L^2(\Omega)} \\ &\quad + \text{osc}(f_2, \mathcal{T}) + \text{osc}(g_2, \mathcal{E}(\Gamma_N)). \end{aligned}$$

from Theorem 4.4 below. The discrete-plus-continuous Korn inequality from Theorem 4.1 below allows the control of the non-symmetric term $\|Du - \Pi_0 Du\|_{L^2(\Omega)}$ in terms of the symmetric stress error $\|\sigma - \mathbb{C}\varepsilon_{\text{NC}}(v_{\text{KS}})\|_{L^2(\Omega)}$. This proves Theorem 2.1.

The remaining parts of this section prove first Theorem 4.1 and then Theorem 4.4.

Theorem 4.1 generalises the discrete Korn inequality from [KS95] in that the underlying function space is $V + \text{KS}(\mathcal{T})$ and not just $\text{KS}(\mathcal{T})$. The Remark 4.1.v of [CF01b] gives the general warning that the Korn inequality in the form of the following Theorem 4.1 is only stated but not proven completely in [BB98].

Theorem 4.1 (discrete-plus-continuous Korn inequality). *For a triangulation \mathcal{T} which fulfils the conditions (c) and (d), any $v_{\text{NC}} \in V + \text{KS}(\mathcal{T})$ satisfies*

$$\|D_{\text{NC}}v_{\text{NC}}\|_{L^2(\Omega)} \lesssim \|\varepsilon_{\text{NC}}(v_{\text{NC}})\|_{L^2(\Omega)}.$$

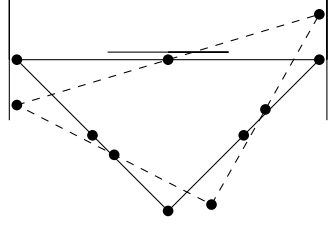
Remark 4.2. The discrete-plus-continuous Korn inequality could be proven for slightly weaker conditions as the conditions (c)–(d) from Subsection 2.3 as in the situation of Figure 2.1d. In those situations, the proof of Theorem 4.1 considers some larger neighbourhoods of the patches. In the situation of Figure 2.1d, it is not guaranteed that those patches do not become arbitrarily large under some refinement strategies and so the constant from the discrete Korn inequality is not uniformly bounded. For the ease of this presentation and the sake of clarity, the slightly stronger versions (c)–(d) are assumed.

The proof of Theorem 4.1 considers a set of vertices $\mathcal{Z} \subseteq \mathcal{N}$ defined by $z \in \mathcal{Z}$ if and only if at least one of the following conditions (i)–(iii) is fulfilled with $\alpha > 0$ from the conditions (c)–(d) of Subsection 2.3.

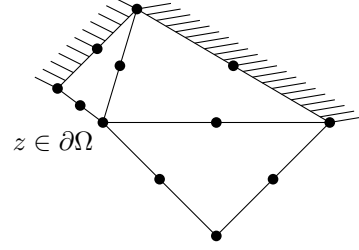
- (i) $z \in \mathcal{N}(\Omega)$,
- (ii) $z \in \mathcal{N}(\partial\Omega)$ with $|v_E(1)| > \alpha$ for all $E \in \mathcal{E}(\omega_z)$ for the nodal patch $\omega_z := \text{int}(\bigcup\{T \in \mathcal{T} \mid z \in T\})$, and if $|\{E \in \mathcal{E}(\Gamma_D \cap \bar{\omega}_z) \mid |v_E(1)| < \alpha\}| = 1$, then $|\{E \in \mathcal{E}(\Gamma_D \cap \bar{\omega}_z) \mid |v_E(1)| > \alpha\}| > 0$,
- (iii) $z \in \mathcal{N}(\partial\Omega)$ and there exists an edge $E \in \mathcal{E}(\omega_z)$ with $\mathcal{N}(E) \subseteq \mathcal{N}(\partial\Omega)$ and $|v_E(1)| < \alpha$, which decomposes the patch ω_z in the two domains ω_1, ω_2 (i.e., ω_1, ω_2 connected with $\bar{\omega}_1 \cap \bar{\omega}_2 = E$ and $\omega_1 \cup \omega_2 \cup \text{int}(E) = \omega_z$). For each of the two domains ω_1 and ω_2 there exists $E_1 \in \mathcal{E}(\partial\omega_1) \cap \mathcal{E}(\Gamma_D)$ and $E_2 \in \mathcal{E}(\partial\omega_2) \cap \mathcal{E}(\Gamma_D)$ on the Dirichlet boundary with $|v_{E_1}(1)| > \alpha$ and $|v_{E_2}(1)| > \alpha$ as depicted in Figure 2.1c.

Recall that the generic multiplicative constants hidden in the notation \lesssim may depend on α .

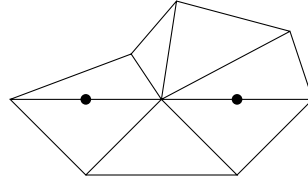
The set \mathcal{Z} contains all interior nodes and some nodes on the boundary, for which some local discrete Korn inequality holds on the nodal patches. The proof of Theorem 4.1 below uses that under the conditions (c)–(d) of Subsection 2.3 the set \mathcal{Z} is large enough to prove the theorem even if that set is empty and the mesh is very coarse (without any interior node). The first step of this proof is the subsequent lemma.



(a) An excluded infinitesimal rigid body motion.



(b) Situation of Figure 4.1a embedded in a triangulation, excluded by condition (c).



(c) Interior patch.

Figure 4.1: Illustration of critical situations for Lemma 4.3.

Lemma 4.3 (characterisation of rigid body motions). *Let \mathcal{T} be a triangulation which fulfils the conditions (c)–(d) of Subsection 2.3 and define \mathcal{Z} as above. Then any $v_{\text{KS}} \in \text{KS}(\mathcal{T})$ with $\varepsilon_{\text{NC}}(v_{\text{KS}}|_{\omega_z}) = 0$ on the nodal patch ω_z for $z \in \mathcal{Z}$ is continuous on ω_z . For $E \in \mathcal{E}(\Omega)$ with $|v_E(1)| \geq \alpha$ any $v_{\text{KS}} \in \text{KS}(\mathcal{T})$ with $\varepsilon_{\text{NC}}(v_{\text{KS}}|_{\omega_E}) = 0$ on the edge-patch $\omega_E := \text{int}(\bigcup\{T \in \mathcal{T} \mid E \in \mathcal{E}(T)\})$ is continuous on ω_E .*

Proof. The critical situation concerns horizontal edges as depicted in Figure 4.1a. For interior nodes the rigid body motions are fixed through two midpoints of those horizontal edges (see Figure 4.1c). For nodes on the boundary condition (iii) guarantees that the rigid body motions are fixed by the boundary conditions. In the case of the edge-patches such critical situations are excluded. \square

Proof of Theorem 4.1. Define $\tilde{\Gamma}_D := \bigcup\{E \in \mathcal{E}(\Gamma_D) \mid |v_E(1)| > \alpha \text{ or there exists } F \in \mathcal{E}(\Gamma_D) \text{ with } F \neq E \text{ and } F \cap E \neq \emptyset\}$. The point of departure is the discrete Korn inequality for piecewise H^1 functions [Bre04, Equation (1.19)]

$$\begin{aligned} & \|D_{\text{NC}} v_{\text{NC}}\|_{L^2(\Omega)} \\ & \lesssim \|\varepsilon_{\text{NC}}(v_{\text{NC}})\|_{L^2(\Omega)} + \|v_{\text{NC}}\|_{L^2(\tilde{\Gamma}_D)} + \sqrt{\sum_{E \in \mathcal{E}(\Omega)} |E|^{-1} \|[v_{\text{NC}}]_E\|_{L^2(E)}^2}. \end{aligned}$$

For any vertex $z \in \mathcal{Z}$ set $\mathcal{T}(z) := \{T \in \mathcal{T} \mid z \in T\}$ the set of all triangles with vertex z and define $\mathcal{E}_z := \{E \in \mathcal{E}(\Omega \cup \tilde{\Gamma}_D) \mid z \in E \text{ and if } E \in \mathcal{E}(\tilde{\Gamma}_D) \text{ and } |v_E(1)| < \alpha \text{ then } |\mathcal{E}(\tilde{\Gamma}_D)| > 1\}$ and let $\omega_z := \text{int}(\cup \mathcal{T}(z))$ be the nodal patch. On $\text{KS}(\mathcal{T}(z)) := \{v_{\text{KS}} \in P_1(\mathcal{T}(z), \mathbb{R}^2) \mid \exists w_{\text{KS}} \in \text{KS}(\mathcal{T}) \text{ s.t. } v_{\text{KS}} = w_{\text{KS}}|_{\omega_z}\}$ the maps

$$\begin{aligned} \rho_1(v_{\text{KS}}) &:= \sqrt{\sum_{E \in \mathcal{E}_z} |E|^{-1} \|[v_{\text{KS}}]_E\|_{L^2(E)}^2} \\ \text{and } \rho_2(v_{\text{KS}}) &:= \inf_{v \in V(\omega_z)} \|\varepsilon_{\text{NC}}(v_{\text{KS}} - v)\|_{L^2(\omega_z)} \end{aligned} \quad (4.1)$$

define two seminorms, where

$$V(\omega_z) := \{w \in L^2(\omega_z; \mathbb{R}^2) \mid \exists v \in V \text{ with } w = v|_{\omega_z}\}.$$

The triangle inequality implies that infimising sequences $v_n \in V(\omega_z)$ in (4.1) are bounded in $H^1(\omega_z; \mathbb{R}^2)$. Since $V(\omega_z)$ is a closed subspace of the reflexive space $H^1(\omega_z; \mathbb{R}^2)$, there exists a subsequence v_{n_k} and a function $v_\infty \in V(\omega_z)$ with $v_{n_k} \rightharpoonup v_\infty$. This and the weak lower semi continuity of the norm $\|\varepsilon(\bullet)\|_{L^2(\omega_z)}$ on $V(\omega_z)$ imply that the infimum is in fact a minimum.

If $\rho_2(v_{\text{KS}}) = 0$ for $v_{\text{KS}} \in \text{KS}(\mathcal{T}(z))$, then there exists some $v \in V(\omega_z)$ with $\varepsilon_{\text{NC}}(v_{\text{KS}}) = \varepsilon(v)$. Therefore, $w_{\text{KS}} := v - v_{\text{KS}} \in P_1(\mathcal{T}(z); \mathbb{R}^2)$ is a piecewise rigid body motion. This implies

$$v \in P_1(\mathcal{T}(z); \mathbb{R}^2) \cap C(\omega_z; \mathbb{R}^2) \subset \text{KS}(\mathcal{T}(z))$$

and therefore $w_{\text{KS}} \in \text{KS}(\mathcal{T}(z))$. Lemma 4.3 implies that $w_{\text{KS}} \in C(\omega_z; \mathbb{R}^2)$ is continuous. Hence, $v_{\text{KS}} = v - w_{\text{KS}} \in C(\omega_z; \mathbb{R}^2)$ and $v_{\text{KS}}|_E \equiv 0$ for $E \in \mathcal{E}_z \cup \tilde{\Gamma}_D$ and therefore $\rho_1(v_{\text{KS}}) = 0$. Since ρ_1 and ρ_2 are seminorms on the finite dimensional space $\text{KS}(\mathcal{T}(z))$, there exists a constant $C(\mathcal{T}(z))$, such that $\rho_1 \leq C(\mathcal{T}(z))\rho_2$. A scaling argument shows, that the constant $C(\mathcal{T}(z))$ is independent of the mesh-size and depends on the minimal angle in $\mathcal{T}(z)$ and on $\alpha > 0$ from the conditions (c)–(d) only.

For $E \in \mathcal{E}(\Omega \cup \tilde{\Gamma}_D)$ with $|v_E(1)| \geq \alpha$, a similar argument shows the inequality $\rho_1 \lesssim \rho_2$ for the two seminorms (of $v_{\text{KS}} \in \text{KS}(\mathcal{T}(z))$)

$$\begin{aligned} \rho_1(v_{\text{KS}}) &:= |E|^{-1/2} \|[v_{\text{KS}}]_E\|_{L^2(E)} \quad \text{and} \\ \rho_2(v_{\text{KS}}) &:= \inf_{v \in V(\omega_E)} \|\varepsilon_{\text{NC}}(v_{\text{KS}} - v)\|_{L^2(\omega_E)}. \end{aligned}$$

Notice that for all $E \in \mathcal{E}(\Omega \cup \tilde{\Gamma}_D)$ with $|v_E(1)| < \alpha$, the conditions (c)–(d) guarantee the existence of a node $z \in \mathcal{Z}$ with $E \in \mathcal{E}_z$. Since the length of edges

$E \in \mathcal{E}(\Gamma_D)$ on the Dirichlet boundary is bounded, $|E| \lesssim 1$, the sum over all vertices $z \in \mathcal{Z}$ and the bounded overlap of the patches show

$$\begin{aligned}
 & \|v_{\text{KS}}\|_{L^2(\tilde{\Gamma}_D)} + \sqrt{\sum_{E \in \mathcal{E}(\Omega)} |E|^{-1} \|[v_{\text{KS}}]_E\|_{L^2(E)}^2} \\
 & \lesssim \sqrt{\sum_{E \in \mathcal{E}(\Omega \cup \tilde{\Gamma}_D)} |E|^{-1} \|[v_{\text{KS}}]_E\|_{L^2(E)}^2} \\
 & \lesssim \sqrt{\sum_{\substack{E \in \mathcal{E}(\Omega \cup \tilde{\Gamma}_D) \\ |v_E(1)| \geq \alpha}} |E|^{-1} \|[v_{\text{KS}}]_E\|_{L^2(E)}^2 + \sum_{z \in \mathcal{Z}} \sum_{E \in \mathcal{E}_z} |E|^{-1} \|[v_{\text{KS}}]_E\|_{L^2(E)}^2} \\
 & \lesssim \inf_{v \in V} \|\varepsilon_{\text{NC}}(v_{\text{KS}} - v)\|_{L^2(\Omega)}.
 \end{aligned} \tag{4.2}$$

For $v_{\text{NC}} \in V + \text{KS}(\mathcal{T})$ and $v \in V$ and $v_{\text{KS}} \in \text{KS}(\mathcal{T})$ with $v_{\text{NC}} = v + v_{\text{KS}}$ it holds $[v_{\text{NC}}]_E = [v_{\text{KS}}]_E$ and $v_{\text{NC}}|_{\Gamma_D} = v_{\text{KS}}|_{\Gamma_D}$. The inequality (4.2) implies

$$\begin{aligned}
 \|v_{\text{NC}}\|_{L^2(\tilde{\Gamma}_D)} + \sqrt{\sum_{E \in \mathcal{E}(\Omega)} |E|^{-1} \|[v_{\text{NC}}]_E\|_{L^2(E)}^2} & \lesssim \inf_{w \in V} \|\varepsilon_{\text{NC}}(v_{\text{KS}} - w)\|_{L^2(\Omega)} \\
 & \leq \|\varepsilon_{\text{NC}}(v_{\text{NC}})\|_{L^2(\Omega)}. \quad \square
 \end{aligned}$$

The remaining part of this section proves Theorem 4.4.

Theorem 4.4. *It holds*

$$\begin{aligned}
 \|\sigma - \sigma_{\text{KS}}\|_{L^2(\Omega)} & \lesssim \|\sigma - \Pi_0 \sigma\|_{L^2(\Omega)} + \|(Du - \Pi_0 Du)(1)\|_{L^2(\Omega)} \\
 & \quad + \text{osc}(f_2, \mathcal{T}) + \text{osc}(g_2, \mathcal{E}(\Gamma_N)).
 \end{aligned}$$

Remark 4.5. It remains as an open question whether or not one can neglect the term $\|(Du - \Pi_0 Du)(1)\|_{L^2(\Omega)}$ in the upper bound in Theorem 4.4; it is not clear how to control this term by the stress error.

The inf-sup-condition from Theorem 4.6 below plays an important role for the independence from λ in the proof of Theorem 4.4.

Theorem 4.6 (inf-sup-condition, [KS95]). *Let \mathcal{T} satisfy the conditions (a)–(b). Then it holds*

$$\|p_0\|_{L^2(\Omega)} \lesssim \sup_{v_{\text{KS}} \in \text{KS}(\mathcal{T}) \setminus \{0\}} \frac{\int_{\Omega} p_0 \operatorname{div}_{\text{NC}} v_{\text{KS}} dx}{\|D_{\text{NC}} v_{\text{KS}}\|_{L^2(\Omega)}} \tag{4.3}$$

for all $p_0 \in P_0(\mathcal{T})$ if $\Gamma_N \neq \emptyset$ and for all $p_0 \in P_0(\mathcal{T})$ with $\int_{\Omega} p_0 dx = 0$ if $\Gamma_N = \emptyset$.

Proof. The first paper [KS95] on this nonconforming finite element method aims at an asymptotic result for sufficiently fine mesh-sizes and therefore reasonably ignores the possibly pathological cases on coarse meshes. Following the arguments of pp. 208–210 in [KS95], one can verify that the condition (a) is stronger than the condition (AD) of p. 198 in [KS95] but avoids the modification of the domain necessary in Step 4 of the proof in [KS95]. In fact, the proof in [KS95] reduces the discrete stability to that on the continuous level but changing the mesh results in changing the domain. One possible critics is that the change of the continuous inf-sup constant with respect to the change of the domain is neglected without a detailed discussion in [KS95]. The conditions (a)–(b) of this paper are sufficient to argue on the original domain in a way analogue to [KS95, p208–210]. Since there is no additional idea in the proof, further details of this technicality are omitted. \square

Proof of Theorem 4.4. The triangle inequality implies that it suffices to consider the difference $\|\Pi_0\sigma - \sigma_{\text{KS}}\|_{L^2(\Omega)}$. The L^2 orthogonal decomposition in the isochoric and deviatoric part reads

$$\|\Pi_0\sigma - \sigma_{\text{KS}}\|_{L^2(\Omega)}^2 = \|\text{dev}(\Pi_0\sigma - \sigma_{\text{KS}})\|_{L^2(\Omega)}^2 + (1/4) \|\text{tr}(\Pi_0\sigma - \sigma_{\text{KS}})1_{2 \times 2}\|_{L^2(\Omega)}^2.$$

For $\Gamma_N = \emptyset$ the homogeneous boundary conditions of u and u_{KS} allow an integration by parts for the second term. The continuity condition $\int_E [u_{\text{KS}}]_E ds = 0$ for all $E \in \mathcal{E}(\Omega)$ leads to

$$\int_{\Omega} \text{tr}(\Pi_0\sigma) dx = 0 = \int_{\Omega} \text{tr}(\sigma_{\text{KS}}) dx, \quad (4.4)$$

i.e. $\text{tr}(\Pi_0\sigma - \sigma_{\text{KS}}) \in P_0(\mathcal{T})/\mathbb{R}$. Theorem 4.6 guarantees for $\Gamma_N = \emptyset$ and $\Gamma_N \neq \emptyset$ the existence of $v_{\text{KS}} \in \text{KS}(\mathcal{T})$ with $\|D_{\text{NC}}v_{\text{KS}}\|_{L^2(\Omega)} = 1$ and

$$\begin{aligned} \|\text{tr}(\Pi_0\sigma - \sigma_{\text{KS}})\|_{L^2(\Omega)} &\lesssim \int_{\Omega} \text{tr}(\Pi_0\sigma - \sigma_{\text{KS}}) \text{div}_{\text{NC}} v_{\text{KS}} dx \\ &= \int_{\Omega} (\Pi_0\sigma - \sigma_{\text{KS}}) : D_{\text{NC}}v_{\text{KS}} dx - \int_{\Omega} \text{dev}(\Pi_0\sigma - \sigma_{\text{KS}}) : D_{\text{NC}}v_{\text{KS}} dx. \end{aligned}$$

The application of Lemma 3.5 to the first term of the right-hand side yields

$$\begin{aligned} \|\text{tr}(\Pi_0\sigma - \sigma_{\text{KS}})\|_{L^2(\Omega)} &\lesssim \|(\sigma - \Pi_0\sigma)(2)\|_{L^2(\Omega)} + \text{osc}(f_2, \mathcal{T}) + \text{osc}(g_2, \mathcal{E}(\Gamma_N)) \\ &\quad + \|\text{dev}(\Pi_0\sigma - \sigma_{\text{KS}})\|_{L^2(\Omega)}. \end{aligned}$$

It remains the analysis of $\|\text{dev}(\Pi_0\sigma - \sigma_{\text{KS}})\|_{L^2(\Omega)}$. Algebraic manipulations show $\text{dev} \mathbb{C}A : \text{dev} \mathbb{C}A \lesssim A : \mathbb{C}A$ for all $A \in \mathbb{R}^{2 \times 2}$. Applied to the above situation this reads

$$\|\text{dev}(\Pi_0\sigma - \sigma_{\text{KS}})\|_{L^2(\Omega)}^2 \lesssim \int_{\Omega} (\Pi_0\sigma - \sigma_{\text{KS}}) : \varepsilon_{\text{NC}}(I_{\text{NC}}u - u_{\text{KS}}) dx. \quad (4.5)$$

The point is, that $\mathbb{C} \operatorname{dev} A$ does not depend on λ . Theorem 3.1 guarantees the existence of $\alpha_{\text{KS}} \in \text{KS}(\mathcal{T})$ and $\beta_{\text{KS}^*} \in \text{KS}^*(\mathcal{T})$ with the property, that $\operatorname{Curl}_{\text{NC}} \beta_{\text{KS}^*} \in P_0(\mathcal{T}; \mathbb{S})$ and $\Pi_0 \sigma - \sigma_{\text{KS}} = \mathbb{C} \varepsilon_{\text{NC}}(\alpha_{\text{KS}}) + \operatorname{Curl}_{\text{NC}} \beta_{\text{KS}^*}$. Lemma 3.5 and 3.6 yield

$$\begin{aligned} & \int_{\Omega} (\Pi_0 \sigma - \sigma_{\text{KS}}) : \varepsilon_{\text{NC}}(I_{\text{NC}} u - u_{\text{KS}}) dx \\ &= \int_{\Omega} \varepsilon_{\text{NC}}(\alpha_{\text{KS}}) : (\Pi_0 \sigma - \sigma_{\text{KS}}) dx + \int_{\Omega} \operatorname{Curl}_{\text{NC}} \beta_{\text{KS}^*} : \varepsilon_{\text{NC}}(I_{\text{NC}} u - u_{\text{KS}}) dx \\ &\lesssim (\|(\Pi_0 \sigma - \sigma)(2)\|_{L^2(\Omega)} + \operatorname{osc}(f_2, \mathcal{T}) + \operatorname{osc}(g_2, \mathcal{E}(\Gamma_N))) \|\nabla_{\text{NC}} \alpha_{\text{KS}}(2)\|_{L^2(\Omega)} \\ &\quad + \|(Du - \Pi_0 Du)(1)\|_{L^2(\Omega)} \|\operatorname{Curl}_{\text{NC}} \beta_{\text{KS}^*}(1)\|_{L^2(\Omega)}. \end{aligned} \tag{4.6}$$

A similar argumentation as in the decomposition of $\Pi_0 \sigma - \sigma_{\text{KS}}$ in the isochoric and the deviatoric part in the beginning of the proof bounds the term $\|\operatorname{Curl}_{\text{NC}} \beta_{\text{KS}^*}(1)\|_{L^2(\Omega)}^2$ by $(\operatorname{Curl}_{\text{NC}} \beta_{\text{KS}^*}, \mathbb{C}^{-1} \operatorname{Curl}_{\text{NC}} \beta_{\text{KS}^*})_{\mathbb{C}^{-1}}$. For this purpose $\operatorname{Curl}_{\text{NC}} \beta_{\text{KS}^*}$ is L^2 orthogonal decomposed in the isochoric and the deviatoric part, i.e.,

$$\begin{aligned} & \|\operatorname{Curl}_{\text{NC}} \beta_{\text{KS}^*}\|_{L^2(\Omega)}^2 \\ &= \|\operatorname{dev}(\operatorname{Curl}_{\text{NC}} \beta_{\text{KS}^*})\|_{L^2(\Omega)}^2 + (1/4) \|\operatorname{tr}(\operatorname{Curl}_{\text{NC}} \beta_{\text{KS}^*}) \mathbf{1}_{2 \times 2}\|_{L^2(\Omega)}^2. \end{aligned} \tag{4.7}$$

For $\Gamma_N = \emptyset$ the function α_{KS} satisfies

$$\begin{aligned} \int_{\Omega} \operatorname{tr}(\mathbb{C} \varepsilon_{\text{NC}}(\alpha_{\text{KS}})) dx &= (2\mu + 2\lambda) \int_{\Omega} \operatorname{div}_{\text{NC}}(\alpha_{\text{KS}}) dx \\ &= (2\mu + 2\lambda) \sum_{E \in \mathcal{E}} \int_E [\alpha_{\text{KS}}]_E \nu_E ds = 0. \end{aligned}$$

It follows with (4.4) $\int_{\Omega} \operatorname{tr}(\operatorname{Curl}_{\text{NC}} \beta_{\text{KS}^*}) dx = 0$. The inf-sup-condition for Kouhia-Stenberg functions, Theorem 4.6, guarantees for $\Gamma_N = \emptyset$ and $\Gamma_N \neq \emptyset$ the existence of $\nu_{\text{KS}} \in \text{KS}(\mathcal{T})$ with $\|D_{\text{NC}} \nu_{\text{KS}}\|_{L^2(\Omega)} = 1$ and

$$\|\operatorname{tr}(\operatorname{Curl}_{\text{NC}} \beta_{\text{KS}^*})\|_{L^2(\Omega)} \lesssim \int_{\Omega} \operatorname{tr}(\operatorname{Curl}_{\text{NC}} \beta_{\text{KS}^*}) \operatorname{div}_{\text{NC}} \nu_{\text{KS}} dx.$$

It follows for $\beta_{\text{KS}^*} = (\beta_{\text{CR}}, \beta_{\text{C}})$ with $\beta_{\text{CR}} \in \text{CR}_N^1(\mathcal{T})$ and $\beta_{\text{C}} \in P_1(\mathcal{T}) \cap C_N(\Omega)$ and $\nu_{\text{KS}} = (\nu_{\text{C}}, \nu_{\text{CR}})$ with $\nu_{\text{C}} \in P_1(\mathcal{T}) \cap C_D(\Omega)$ and $\nu_{\text{CR}} \in \text{CR}_D^1(\mathcal{T})$, that

$$\begin{aligned} & \|\operatorname{tr}(\operatorname{Curl}_{\text{NC}} \beta_{\text{KS}^*})\|_{L^2(\Omega)} \\ &\lesssim \int_{\Omega} (\operatorname{Curl}_{\text{NC}} \beta_{\text{KS}^*} - \operatorname{dev} \operatorname{Curl}_{\text{NC}} \beta_{\text{KS}^*}) : D_{\text{NC}} \nu_{\text{KS}} dx \\ &\leq \|\operatorname{dev} \operatorname{Curl}_{\text{NC}} \beta\|_{L^2(\Omega)} \|D_{\text{NC}} \nu_{\text{KS}}\|_{L^2(\Omega)} \\ &\quad + \int_{\Omega} \operatorname{Curl}_{\text{NC}} \beta_{\text{CR}} \cdot \nabla \nu_{\text{C}} dx + \int_{\Omega} \operatorname{Curl} \beta_{\text{C}} \cdot \nabla_{\text{NC}} \nu_{\text{CR}} dx. \end{aligned} \tag{4.8}$$

Since $\nabla_{\mathbf{V}_C} \boldsymbol{\tau}_E$ vanishes on Γ_D , an integration by parts leads to

$$\begin{aligned} & \int_{\Omega} \text{Curl}_{\text{NC}} \boldsymbol{\beta}_{\text{CR}} \cdot \nabla_{\mathbf{V}_C} dx \\ &= \sum_{E \in \mathcal{E}(\Omega)} \int_E [\boldsymbol{\beta}_{\text{CR}}]_E ds \nabla_{\mathbf{V}_C} \cdot \boldsymbol{\tau}_E + \sum_{E \in \mathcal{E}(\Gamma_N)} \int_E \boldsymbol{\beta}_{\text{CR}} ds \nabla_{\mathbf{V}_C} \cdot \boldsymbol{\tau}_E = 0. \end{aligned}$$

Since $\nabla \boldsymbol{\beta}_C \cdot \boldsymbol{\tau}_E$ vanishes on $E \in \mathcal{E}(\Gamma_N)$,

$$\begin{aligned} & \int_{\Omega} \text{Curl} \boldsymbol{\beta}_C \cdot \nabla_{\text{NC}} v_{\text{CR}} dx \\ &= \sum_{E \in \mathcal{E}(\Gamma_D)} \int_E v_{\text{CR}} ds (\nabla \boldsymbol{\beta}_C \cdot \boldsymbol{\tau}_E) + \sum_{E \in \mathcal{E}(\Omega)} \int_E [v_{\text{CR}}]_E ds (\nabla \boldsymbol{\beta}_C \cdot \boldsymbol{\tau}_E) = 0. \end{aligned}$$

Together with (4.7)–(4.8) it follows

$$\|\text{tr}(\text{Curl}_{\text{NC}} \boldsymbol{\beta}_{\text{KS}^*})\|_{L^2(\Omega)} + \|\text{Curl}_{\text{NC}} \boldsymbol{\beta}_{\text{KS}^*}\|_{L^2(\Omega)} \lesssim \|\text{dev} \text{Curl}_{\text{NC}} \boldsymbol{\beta}_{\text{KS}^*}\|_{L^2(\Omega)}$$

Since $\text{dev} \mathbb{C}A : \text{dev} \mathbb{C}A \lesssim A : \mathbb{C}A$ for all $A \in \mathbb{R}^{2 \times 2}$ it follows as above

$$\|\text{Curl}_{\text{NC}} \boldsymbol{\beta}_{\text{KS}^*}\|_{L^2(\Omega)}^2 \lesssim (\text{Curl}_{\text{NC}} \boldsymbol{\beta}_{\text{KS}^*}, \text{Curl}_{\text{NC}} \boldsymbol{\beta}_{\text{KS}^*})_{\mathbb{C}^{-1}}.$$

Theorem 4.1 implies

$$\|\nabla_{\text{NC}} \boldsymbol{\alpha}_{\text{KS}}(2)\|_{L^2(\Omega)}^2 \lesssim \|\boldsymbol{\varepsilon}_{\text{NC}}(\boldsymbol{\alpha}_{\text{KS}})\|_{L^2(\Omega)}^2 \lesssim (\mathbb{C}\boldsymbol{\varepsilon}_{\text{NC}}(\boldsymbol{\alpha}_{\text{KS}}), \mathbb{C}\boldsymbol{\varepsilon}_{\text{NC}}(\boldsymbol{\alpha}_{\text{KS}}))_{\mathbb{C}^{-1}}.$$

The orthogonality of the decomposition $\Pi_0 \boldsymbol{\sigma} - \boldsymbol{\sigma}_{\text{KS}} = \mathbb{C}\boldsymbol{\varepsilon}_{\text{NC}}(\boldsymbol{\alpha}_{\text{KS}}) + \text{Curl}_{\text{NC}} \boldsymbol{\beta}_{\text{KS}^*}$ with respect to $(\bullet, \bullet)_{\mathbb{C}^{-1}}$ implies together with the above estimate that

$$\begin{aligned} & \|\nabla_{\text{NC}} \boldsymbol{\alpha}_{\text{KS}}(2)\|_{L^2(\Omega)} + \|\text{Curl}_{\text{NC}} \boldsymbol{\beta}_{\text{KS}^*}\|_{L^2(\Omega)} \\ & \lesssim \left(\int_{\Omega} (\Pi_0 \boldsymbol{\sigma} - \boldsymbol{\sigma}_{\text{KS}}) : \boldsymbol{\varepsilon}_{\text{NC}}(I_{\text{NC}} u - u_{\text{KS}}) dx \right)^{1/2}. \end{aligned}$$

Inequality (4.6) proves

$$\begin{aligned} & \left(\int_{\Omega} (\Pi_0 \boldsymbol{\sigma} - \boldsymbol{\sigma}_{\text{KS}}) : \boldsymbol{\varepsilon}_{\text{NC}}(I_{\text{NC}} u - u_{\text{KS}}) dx \right)^{1/2} \\ & \lesssim \|(\Pi_0 \boldsymbol{\sigma} - \boldsymbol{\sigma})(2)\|_{L^2(\Omega)} + \text{osc}(f_2, \mathcal{T}) + \text{osc}(g_2, \mathcal{E}(\Gamma_N)) \\ & \quad + \|(Du - \Pi_0 Du)(1)\|_{L^2(\Omega)}. \end{aligned}$$

This and (4.5) conclude the proof of Theorem 4.4. \square

5 Proof of Theorems 2.3 and 2.4

The first part of this section proves Theorem 2.3 while the second one proves Theorem 2.4.

The proof of Theorem 2.3 is based on the following lemma. It corresponds to Lemma 3.5 for Crouzeix-Raviart functions.

Lemma 5.1. $v_{\text{CR}} \in V_{\text{CR}}(\mathcal{T})$ satisfies

$$\int_{\Omega} (\tilde{\sigma} - \tilde{\sigma}_{\text{CR}}) : D_{\text{NC}} v_{\text{CR}} dx \lesssim \left(\|\tilde{\sigma} - \Pi_0 \tilde{\sigma}\|_{L^2(\Omega)} + \text{osc}(f, \mathcal{T}) \right) \|D_{\text{NC}} v_{\text{CR}}\|_{L^2(\Omega)}.$$

Proof. Lemma 3.3 implies with a piecewise Poincaré inequality for J_3 (applied componentwise)

$$\begin{aligned} \int_{\Omega} (\tilde{\sigma} - \tilde{\sigma}_{\text{CR}}) : D_{\text{NC}} v_{\text{CR}} dx &= \int_{\Omega} (\tilde{\mathbb{C}}(D_{\text{NC}} I_{\text{NC}} u) - \tilde{\sigma}_{\text{CR}}) : D_{\text{NC}} v_{\text{CR}} dx \\ &= \int_{\Omega} f \cdot (J_3 v_{\text{CR}} - v_{\text{CR}}) dx + \int_{\Omega} (\tilde{\mathbb{C}}(D_{\text{NC}} I_{\text{NC}} u) - \tilde{\sigma}) : DJ_3 v_{\text{CR}} dx \\ &\leq \|h_{\mathcal{T}}(f - \Pi_0 f)\|_{L^2(\Omega)} \|J_3 v_{\text{CR}} - v_{\text{CR}}\|_{L^2(\Omega)} \\ &\quad + \|\Pi_0 \tilde{\sigma} - \tilde{\sigma}\|_{L^2(\Omega)} \|DJ_3 v_{\text{CR}}\|_{L^2(\Omega)} \\ &\lesssim \text{osc}(f, \mathcal{T}) \|D_{\text{NC}} v_{\text{CR}}\|_{L^2(\Omega)} + \|\Pi_0 \tilde{\sigma} - \tilde{\sigma}\|_{L^2(\Omega)} \|D_{\text{NC}} v_{\text{CR}}\|_{L^2(\Omega)} \quad \square \end{aligned} \tag{5.1}$$

Proof of Theorem 2.3. The point of departure is an inequality of [CR12, Lemma 3.8],

$$\|\tilde{\sigma} - \tilde{\sigma}_{\text{CR}}\|_{L^2(\Omega)}^2 \lesssim \int_{\Omega} (\tilde{\sigma} - \tilde{\sigma}_{\text{CR}}) : (Du - D_{\text{NC}} u_{\text{CR}}) dx + \|h_{\mathcal{T}} f\|_{L^2(\Omega)}^2. \tag{5.2}$$

Define the bubble function $b_T := (\varphi_T, \varphi_T) \in P_3(\mathcal{T}; \mathbb{R}^2)$ with φ_T as in the proof of Lemma 3.5. The property $\int_T b_T dx \approx |T|$ implies

$$\begin{aligned} \|h_{\mathcal{T}} f\|_{L^2(T)} &\leq \text{osc}(f, T) + \|h_{\mathcal{T}} \Pi_0 f\|_{L(T)} \\ &\approx \text{osc}(f, T) + \left| \int_T b_T \cdot \Pi_0 f dx \right|. \end{aligned}$$

The scaling $\|b_T\|_{L^2(T)} \approx h_{\mathcal{T}} |T|$ and an integration by parts show

$$\begin{aligned} \left| \int_T b_T \cdot \Pi_0 f dx \right| &\leq \|b_T\|_{L^2(T)} \|f - \Pi_0 f\|_{L^2(T)} + \left| \int_T b_T \cdot f dx \right| \\ &\lesssim \text{osc}(f, T) + \left| \int_T Db_T : (\sigma - \Pi_0 \sigma) dx \right|. \end{aligned}$$

Since $\|Db_T\|_{L^2(T)} \approx 1$ and $(A + A^\top) : (A + A^\top) \leq 4A : A$ it follows

$$\begin{aligned} \left| \int_T Db_T : (\boldsymbol{\sigma} - \Pi_0 \boldsymbol{\sigma}) dx \right| &\lesssim \|\boldsymbol{\sigma} - \Pi_0 \boldsymbol{\sigma}\|_{L^2(T)} \\ &\leq \|\tilde{\boldsymbol{\sigma}} - \Pi_0 \tilde{\boldsymbol{\sigma}}\|_{L^2(T)}. \end{aligned}$$

Altogether

$$\|h_T f\|_{L^2(T)} \leq \text{osc}(f, T) + \|\tilde{\boldsymbol{\sigma}} - \Pi_0 \tilde{\boldsymbol{\sigma}}\|_{L^2(T)}.$$

This, (5.2) and Lemma 5.1 imply

$$\begin{aligned} &\|\tilde{\boldsymbol{\sigma}} - \tilde{\boldsymbol{\sigma}}_{\text{CR}}\|_{L^2(\Omega)}^2 \\ &\lesssim \int_{\Omega} (\tilde{\boldsymbol{\sigma}} - \Pi_0 \tilde{\boldsymbol{\sigma}}) : (Du - \Pi_0 Du) dx + \int_{\Omega} (\tilde{\boldsymbol{\sigma}} - \tilde{\boldsymbol{\sigma}}_{\text{CR}}) : D_{\text{NC}}(I_{\text{NC}}u - u_{\text{CR}}) dx \\ &\quad + \text{osc}^2(f, \mathcal{T}) + \|\tilde{\boldsymbol{\sigma}} - \Pi_0 \tilde{\boldsymbol{\sigma}}\|_{L^2(\Omega)}^2 \\ &\lesssim \|\tilde{\boldsymbol{\sigma}} - \Pi_0 \tilde{\boldsymbol{\sigma}}\|_{L^2(\Omega)}^2 + \text{osc}^2(f, \mathcal{T}) \\ &\quad + (\|\tilde{\boldsymbol{\sigma}} - \Pi_0 \tilde{\boldsymbol{\sigma}}\|_{L^2(\Omega)} + \text{osc}(f, \mathcal{T})) \|D_{\text{NC}}(I_{\text{NC}}u - u_{\text{CR}})\|_{L^2(\Omega)}, \end{aligned}$$

where the last inequality follows from $\|Du - \Pi_0 Du\|_{L^2(\Omega)} \leq \|\tilde{\boldsymbol{\sigma}} - \Pi_0 \tilde{\boldsymbol{\sigma}}\|_{L^2(\Omega)}$. The Young inequality $2ab \leq \alpha a^2 + \alpha^{-1} b^2$ for $\alpha > 0$ implies

$$\begin{aligned} &(\|\tilde{\boldsymbol{\sigma}} - \Pi_0 \tilde{\boldsymbol{\sigma}}\|_{L^2(\Omega)} + \text{osc}(f, \mathcal{T})) \|D_{\text{NC}}(I_{\text{NC}}u - u_{\text{CR}})\|_{L^2(\Omega)} \\ &\leq 1/(4\alpha) (\|\tilde{\boldsymbol{\sigma}} - \Pi_0 \tilde{\boldsymbol{\sigma}}\|_{L^2(\Omega)} + \text{osc}(f, \mathcal{T}))^2 + \alpha \|D_{\text{NC}}(I_{\text{NC}}u - u_{\text{CR}})\|_{L^2(\Omega)}^2. \end{aligned}$$

For sufficiently small α the last term is absorbed. It follows

$$\|\tilde{\boldsymbol{\sigma}} - \tilde{\boldsymbol{\sigma}}_{\text{CR}}\|_{L^2(\Omega)} \lesssim \|\tilde{\boldsymbol{\sigma}} - \Pi_0 \tilde{\boldsymbol{\sigma}}\|_{L^2(\Omega)} + \text{osc}(f, \mathcal{T}). \quad \square$$

The remaining parts of this section are devoted to the proof of Theorem 2.4, which is based on the following proposition.

Proposition 5.2. *For $u_{\text{KS}} \in \text{KS}(\mathcal{T})$ and $1 \lesssim \lambda$ it holds*

$$\min_{v_{\text{C}} \in V_{\text{C}}(\mathcal{T})} \|u_{\text{KS}} - v_{\text{C}}\|_{\text{NC}} \lesssim \lambda^{1/2} \min_{v \in V} \|u_{\text{KS}} - v\|_{\text{NC}}.$$

Proof. The arguments of [CEHL12, Theorem 5.1] prove the crucial point, namely

$$\min_{v_{\text{C}} \in V_{\text{C}}(\mathcal{T})} \|D_{\text{NC}}(v_{\text{KS}} - v_{\text{C}})\|_{L^2(\Omega)} \approx \min_{v \in V} \|D_{\text{NC}}(v_{\text{KS}} - v)\|_{L^2(\Omega)}.$$

(This is proven for scalar functions and the pure Dirichlet problem in [CEHL12] but the local arguments in the proof are still valid for the weaker boundary conditions and for two components.) The estimate

$$\|v_{\text{KS}}\|_{\text{NC}} \lesssim \lambda^{1/2} \|\varepsilon_{\text{NC}}(v_{\text{KS}})\|_{L^2(\Omega)} \leq \lambda^{1/2} \|D_{\text{NC}} v_{\text{KS}}\|_{L^2(\Omega)}$$

and

$$\|D_{\text{NC}}(v_{\text{KS}} - v)\|_{L^2(\Omega)} \leq \|v_{\text{KS}} - v\|_{\text{NC}}$$

conclude the proof of the proposition. \square

Proof of Theorem 2.4. The proof follows in three steps.

Step 1. The inclusion $V_{\text{C}}(\mathcal{T}) \subset \text{KS}(\mathcal{T})$ and Galerkin orthogonality show together with Proposition 5.2

$$\begin{aligned} \|u_{\text{KS}} - u_{\text{C}}\|_{\text{NC}} &\leq \min_{v_{\text{C}} \in V_{\text{C}}(\mathcal{T})} \|u_{\text{KS}} - v_{\text{C}}\|_{\text{NC}} \\ &\lesssim \lambda^{1/2} \min_{v \in V} \|u_{\text{KS}} - v\| \leq \lambda^{1/2} \|u - u_{\text{KS}}\|. \end{aligned}$$

This implies the following inequality for the energy norm

$$\|u - u_{\text{C}}\| \leq \|u - u_{\text{KS}}\|_{\text{NC}} + \|u_{\text{C}} - u_{\text{KS}}\|_{\text{NC}} \lesssim (1 + \lambda^{1/2}) \|u - u_{\text{KS}}\|_{\text{NC}}.$$

Since $|\mathbb{C}A|^2 \lesssim \lambda(A : \mathbb{C}A)$ it follows

$$\|\sigma - \sigma_{\text{C}}\|_{L^2(\Omega)} \lesssim \lambda^{1/2} \|u - u_{\text{C}}\| \lesssim \lambda \|u - u_{\text{KS}}\|_{\text{NC}} \lesssim \lambda \|\sigma - \sigma_{\text{KS}}\|_{L^2(\Omega)}.$$

Step 2. The inequalities

$$\begin{aligned} \|\sigma - \sigma_{\text{KS}}\|_{L^2(\Omega)} &\lesssim \|\sigma - \sigma_{\text{C}}\|_{L^2(\Omega)} + \text{osc}(f_2, \mathcal{T}) + \text{osc}(g_2, \mathcal{E}(\Gamma_N)), \\ \|\sigma - \sigma_{\text{KS}}\|_{L^2(\Omega)} &\lesssim \|\tilde{\sigma} - \tilde{\sigma}_{\text{CR}}\|_{L^2(\Omega)} + \text{osc}(f_2, \mathcal{T}) \quad (\text{if } \Gamma_D = \partial\Omega) \end{aligned}$$

are direct consequences of Theorem 2.1 and 4.4.

Step 3. The inequality $(A + A^\top) : (A + A^\top) \leq 4A : A$ implies

$$(\sigma - \sigma_{\text{CR}}) : (\sigma - \sigma_{\text{CR}}) \lesssim (\tilde{\sigma} - \tilde{\sigma}_{\text{CR}}) : (\tilde{\sigma} - \tilde{\sigma}_{\text{CR}}).$$

From Theorem 4.1 it follows for $\tilde{\sigma}_{\text{KS}} := \tilde{\mathbb{C}}D_{\text{NC}}u_{\text{KS}}$

$$\begin{aligned}
 & \|\tilde{\sigma} - \tilde{\sigma}_{\text{KS}}\|_{L^2(\Omega)}^2 \\
 &= \mu^2 \|D_{\text{NC}}(u - u_{\text{KS}})\|_{L^2(\Omega)}^2 \\
 &\quad + (2\mu(\lambda + \mu) + (\lambda + \mu)^2) \|\text{div}_{\text{NC}}(u - u_{\text{KS}})\|_{L^2(\Omega)}^2 \\
 &\lesssim 4\mu^2 \|\varepsilon_{\text{NC}}(u - u_{\text{KS}})\|_{L^2(\Omega)}^2 + (4\mu\lambda + \lambda^2) \|\text{div}_{\text{NC}}(u - u_{\text{KS}})\|_{L^2(\Omega)}^2 \\
 &= \|\sigma - \sigma_{\text{KS}}\|_{L^2(\Omega)}^2.
 \end{aligned}$$

Altogether,

$$\begin{aligned}
 \|\sigma - \sigma_{\text{CR}}\|_{L^2(\Omega)} &\lesssim \|\tilde{\sigma} - \tilde{\sigma}_{\text{CR}}\|_{L^2(\Omega)} \\
 &\lesssim \|\tilde{\sigma} - \tilde{\sigma}_{\text{KS}}\|_{L^2(\Omega)} + \text{osc}(f, \mathcal{T}) \\
 &\lesssim \|\sigma - \sigma_{\text{KS}}\|_{L^2(\Omega)} + \text{osc}(f, \mathcal{T}).
 \end{aligned}$$

This concludes the proof of Theorem 2.4. □

6 Numerical Investigations

This section provides numerical evidence that the claimed equivalence of σ_{CR} and σ_{KS} is independent of the parameter λ for the pure Dirichlet problem in linear elasticity and that the dependence of the equivalence constants in (1.1) on $\lambda = 1.6 \times 10^k$ for $k = 6, 7, 8, 9$ cannot be improved.

6.1 Preliminaries

Throughout this section, the elastic modulus is $E = 10^5$ and the Poisson ratio varies between $\nu = 0.4, 0.49, 0.499, 0.4999$ with corresponding values of $\mu = E/(2(1 + \nu))$ and $\lambda = E\nu/((1 + \nu)(1 - 2\nu)) = 1.6 \times 10^k$ for $k = 6, 7, 8, 9$. The initial triangulations \mathcal{T}_0 of all four numerical examples are depicted in Figures 6.1 and 6.3. The discrete problems are solved on a sequence of triangulations \mathcal{T}_ℓ obtained by successive red-refinements; a red-refinement of a triangle subdivides each triangle into four congruent sub-triangles via straight lines through the edges' midpoints as depicted in Figure 6.1a.

Since the error is known only in the first example, the averaging error estimator defined in [CF01a, Eqn (2.17)] serves as an error indicator. Although the proofs of efficiency and reliability from [CF01a] provide no information about the efficiency and reliability constants, there is numerical evidence that the averaging error estimator often yields results very close to the exact error [CF01a]. The first

example confirms this observation and so partly justifies the use of this error estimator for the further examples. Let $|T|$ denote the area of a triangle $T \in \mathcal{T}$ and τ_E the tangent of an edge $E \in \mathcal{E}$. The residual error estimators

$$\begin{aligned} \eta_C(u_C) &:= \left(\sum_{T \in \mathcal{T}} \left(|T| \|f\|_{L^2(T)}^2 + |T|^{1/2} \sum_{E \in \mathcal{E}(T) \setminus \mathcal{E}(\Gamma_D)} \|[\sigma_C]_E \nu_E\|_{L^2(E)}^2 \right) \right)^{1/2} \\ \eta_{CR}(u_{CR}) &:= \left(\sum_{T \in \mathcal{T}} \left(|T| \|f\|_{L^2(T)}^2 + |T|^{1/2} \sum_{E \in \mathcal{E}(T) \setminus \mathcal{E}(\Gamma_N)} \|[D_{NC} u_{CR}]_E \tau_E\|_{L^2(E)}^2 \right) \right)^{1/2} \\ \eta_{KS}(u_{KS}) &:= \left(\sum_{T \in \mathcal{T}} \left(|T| \|f\|_{L^2(T)}^2 + |T|^{1/2} \sum_{E \in \mathcal{E}(T) \setminus \mathcal{E}(\Gamma_N)} \|[D_{NC} u_{KS}]_E \tau_E\|_{L^2(E)}^2 \right. \right. \\ &\quad \left. \left. + |T|^{1/2} \sum_{E \in \mathcal{E}(T) \setminus \mathcal{E}(\Gamma_D)} \|(1, 0) \cdot ([\sigma_{KS}]_E \nu_E)\|_{L^2(E)}^2 \right) \right)^{1/2} \end{aligned}$$

for CFEM, CR-NCFEM and KS-NCFEM are reliable and efficient [CF01a, CR12]. In contrast to [CF01a], the normal jump of the second component of the stress is omitted for KS-NCFEM in the spirit of [DDP95].

A close investigation on the dependency on the parameter λ for $\nu = 0.4, 0.49, 0.499$ and 0.4999 in the comparison result (1.1) considers the quotients

$$q(\nu, \ell) := \|\sigma_\nu - \sigma_C^{\ell, \nu}\|_{L^2(\Omega)} / \|\sigma_\nu - \sigma_{KS}^{\ell, \nu}\|_{L^2(\Omega)} \quad \text{for } \ell = 1, \dots, 9. \quad (6.1)$$

Here and in Subsection 6.2 and 6.4, σ_ν denotes the exact stress for the Poisson ratio ν and $\sigma_C^{\ell, \nu}$ and $\sigma_{KS}^{\ell, \nu}$ denote the discrete stresses of CFEM and KS-NCFEM for the Poisson ratio ν and the ℓ -th times red-refined triangulation $\mathcal{T}_\ell := \text{red}^{(\ell)}(\mathcal{T}_0)$. (For the experiment from Subsection 6.4 the quotients are approximated by the corresponding values of the averaging error estimator.)

6.2 Academic Example

Under homogeneous pure Dirichlet boundary conditions, the unit square $\Omega = (0, 1)^2$ is loaded with the applied force

$$f(x, y) = \begin{pmatrix} -2\mu\pi^3 \cos(\pi y) \sin(\pi y) (2 \cos(2\pi x) - 1) \\ 2\mu\pi^3 \cos(\pi x) \sin(\pi x) (2 \cos(2\pi y) - 1) \end{pmatrix}$$

(written as a function of the coordinates x and y) so that (2.1) leads to the exact smooth solution

$$u(x, y) = \begin{pmatrix} \pi \cos(\pi y) \sin^2(\pi x) \sin(\pi y) \\ -\pi \cos(\pi x) \sin^2(\pi y) \sin(\pi x) \end{pmatrix}.$$

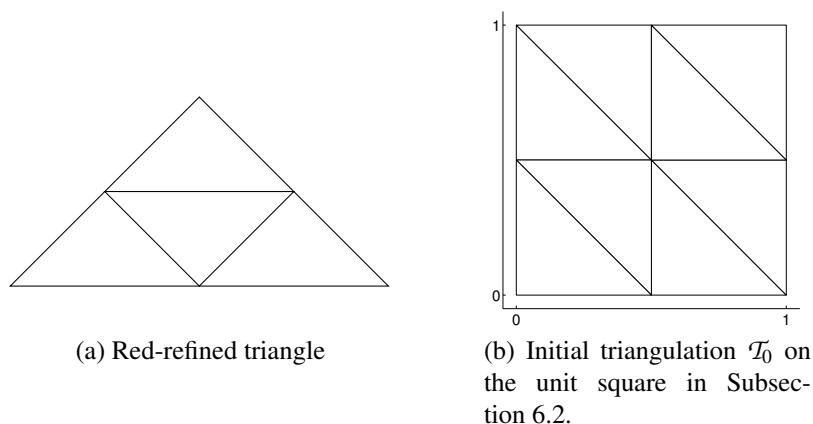


Figure 6.1: Red-refined triangle and the initial triangulation \mathcal{T}_0 of Subsection 6.2.

Given the initial mesh \mathcal{T}_0 of Figure 6.1b with one interior node and 8 interior edges, the three FEMs with the number ndof of degrees of freedom lead on each triangulation \mathcal{T}_ℓ to the discrete stresses $\sigma_C, \sigma_{CR}, \sigma_{KS}$; on the level zero, for instance, $\text{ndof} = 2$ for CFEM, $\text{ndof} = 16$ for CR-NCFEM, and $\text{ndof} = 9$ for KS-NCFEM. The convergence history plot of Figure 6.2 displays various errors and error estimators versus the number of degrees of freedom (ndof) for the Poisson ratios $\nu = 0.4$ (red), 0.49 (blue), 0.499 (green), 0.4999 (cyan) for the three FEMs.

The graphs of the averaging error estimators and the exact error of CR-NCFEM and KS-NCFEM for all values of ν lie on top of each other, as well as the values of the residual error estimator for KS-NCFEM and also the values of the residual error estimator for CR-NCFEM.

For the initial triangulation \mathcal{T}_0 of Figure 6.1b with two degrees of freedom in CFEM, the averaging error estimator strongly underestimates and is omitted. Apart from that case, the values of the averaging error estimator are very close to the exact error. This example therefore serves as an empirical validation of the averaging error estimator in the following examples where it is expected to indicate the (unknown) errors in high accuracy.

Equivalent convergence rates are observed for all three FEMs with a strong dependency on λ for CFEM while the errors in KS-NCFEM and CR-NCFEM are of similar size. Table 6.1 displays the quotients (6.1) and reveals a linear dependency on λ . This is clear numerical evidence that the dependence of λ in the first estimate of (1.1) and in Theorem 2.4 is sharp.

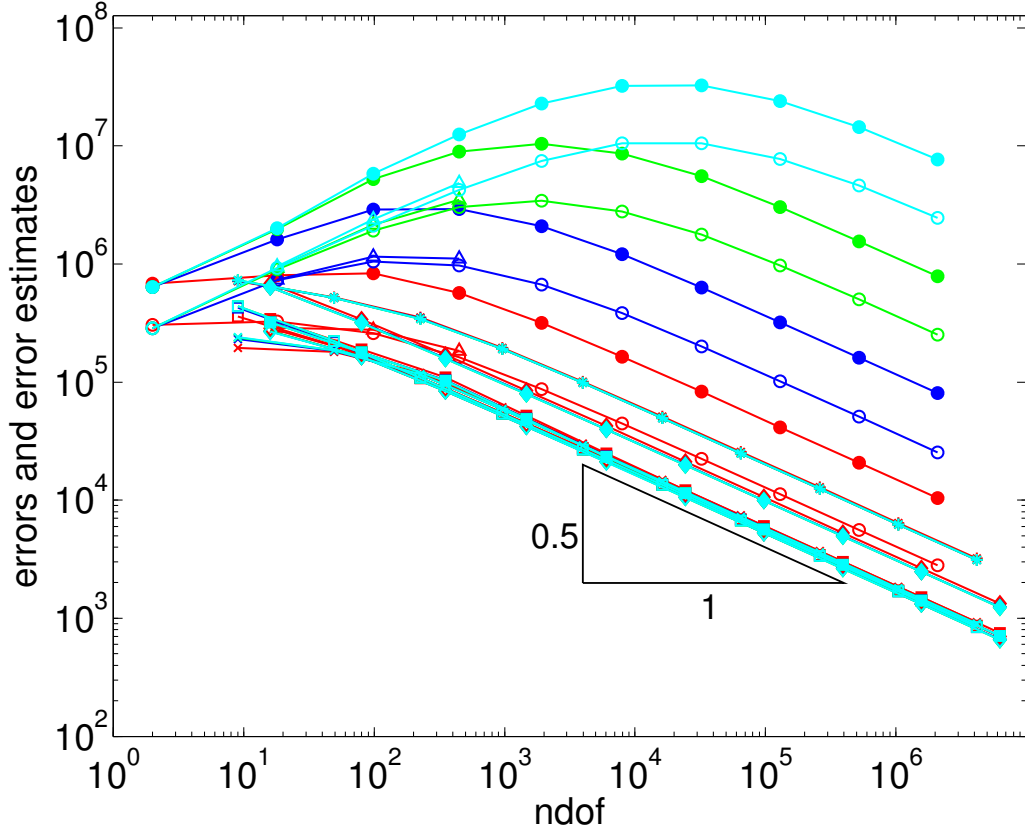


Figure 6.2: Estimated errors of CFEM (residual estimator (\bullet), averaging estimator (\triangle), and exact error (\circ)), CR-NCFEM (residual estimator (\blacklozenge), averaging estimator (\blacksquare), and exact error (\diamond)), and KS-NCFEM (residual estimator ($*$), averaging estimator (\times), and exact error (\square)) for $\nu = 0.4$ (red), 0.49 (blue), 0.499 (green), 0.4999 (cyan) on uniform red-refined meshes for the unit square from Subsection 6.2.

Table 6.1: Quotient $q(\nu, \ell)$ from (6.1) for CFEM and KS-NCFEM in Subsection 6.2

$\nu =$	$\ell = 1$	2	3	4	5	6	7	8	9
0.4	0.8461	1.588	2.411	2.947	3.165	3.229	3.246	3.250	3.251
0.49	0.6717	3.327	9.667	17.95	24.84	28.46	29.71	30.05	30.14
0.499	0.6498	4.053	17.61	56.26	127.5	207.0	264.0	289.3	297.3
0.4999	0.6476	4.150	19.52	78.29	277.7	778.8	1556	2301	2755

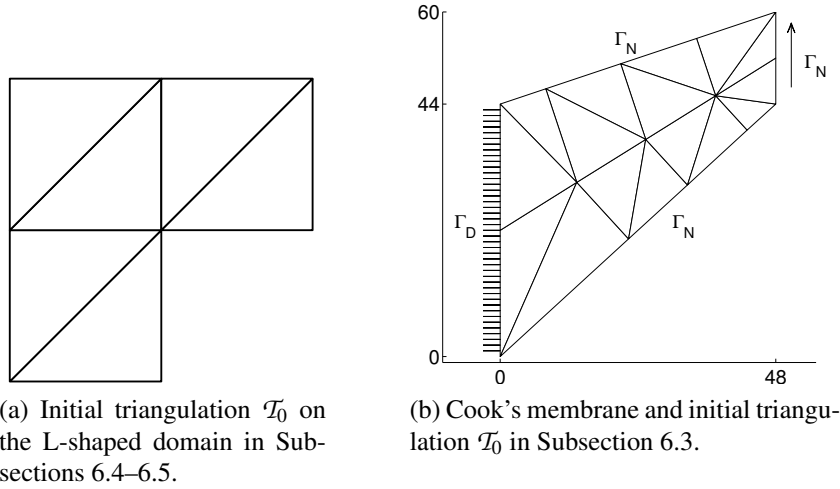


Figure 6.3: Initial triangulations \mathcal{T}_0 in Subsections 6.3–6.5.

6.3 Cook's Membrane Benchmark

This benchmark in linear elasticity concerns the domain Ω of Figure 6.3b with the vertices $(0, 0)$, $(48, 44)$, $(48, 60)$, $(0, 44)$ and the Dirichlet boundary $\Gamma_D := \text{conv}\{(0, 0), (0, 44)\}$ and $\Gamma_N := \partial\Omega \setminus \Gamma_D$. The applied forces are $f \equiv 0$ in Ω and $g(x) = (0, 1)$ if $x(1) = 48$ on the right vertical edge of $\partial\Omega$ while $g \equiv 0$ on the remaining two parts of Γ_N . The Neumann boundary of the problem excludes CR-NCFEM. The estimated errors of CFEM and KS-NCFEM are plotted against the number of degrees of freedom in Figure 6.4. For $\nu = 0.49, 0.499, 0.4999$ the values of the averaging error estimator for KS-NCFEM lie on top of each other, as well as the values of the residual error estimator for KS-NCFEM.

The locking behaviour of CFEM and the robustness of KS-NCFEM (with respect to λ) is clearly visible in the sense that the preasymptotic range for CFEM is so big that it covers the full range of our computational feasibilities with the effect that for $\nu = 0.4999$ all the computational values are not even better than the initial stress approximation (relative to the L^2 norm).

Notice that the jump of the boundary conditions at the vertex $(0, 44)$ causes a solution $u \notin H^2(\Omega; \mathbb{R}^2)$ in agreement of the reduced convergence rates (under uniform mesh-refinement) and, hence, the conditions of [KS95] are violated.

6.4 L-shaped Domain Without Locking

This example shows that the equivalence constant in the second inequality of (1.1) cannot be replaced by any negative power of λ . The underlying domain of this

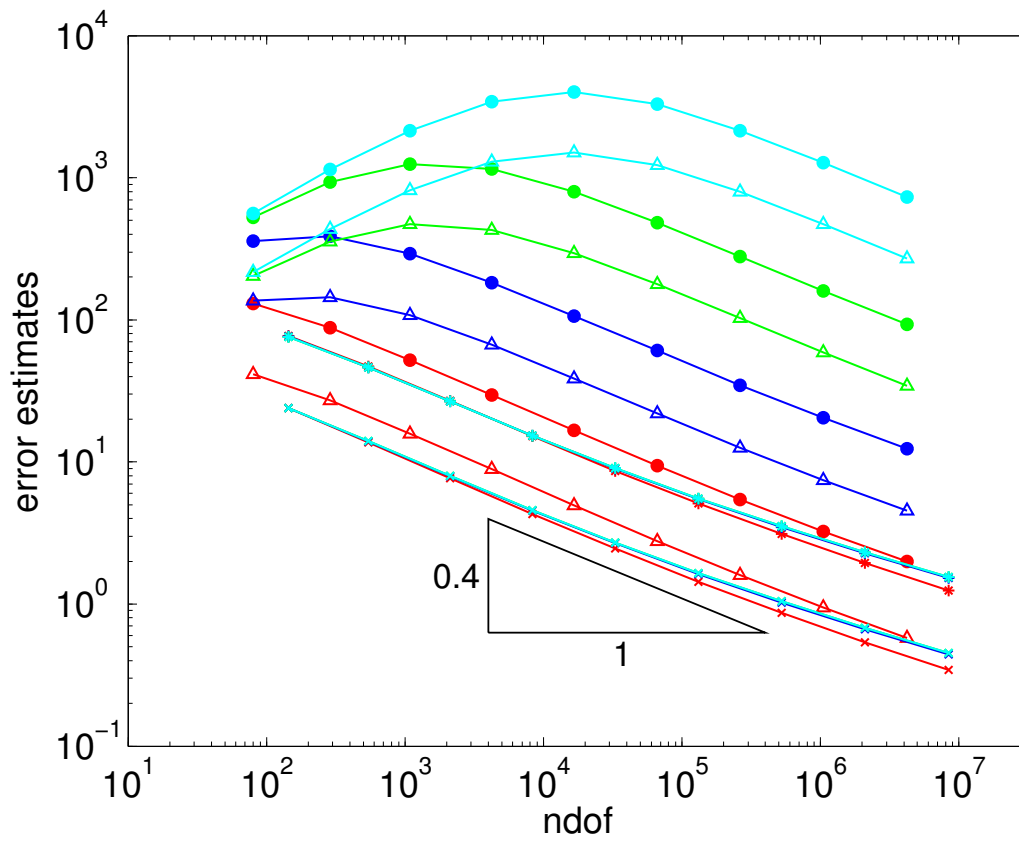


Figure 6.4: Estimated errors of CFEM (residual estimator (●) and averaging estimator (△)) and KS-NCFEM (residual estimator (*) and averaging estimator (×)) for $\nu = 0.4$ (red), 0.49 (blue), 0.499 (green), 0.4999 (cyan) on uniform red-refined meshes for Cook's Membrane from Subsection 6.3.

Table 6.2: Approximated quotient $q(\mathbf{v}, \ell)$ from (6.1) for CFEM and KS-NCFEM in Subsection 6.4

$\mathbf{v} =$	$\ell = 1$	2	3	4	5	6	7	8
0.4	1.123	1.502	1.762	1.931	2.037	2.097	2.123	2.118
0.49	1.348	2.057	2.705	3.291	3.807	4.252	4.641	4.989
0.499	1.371	2.130	2.790	3.342	3.869	4.393	4.882	5.334
0.4999	1.373	2.138	2.803	3.336	3.783	4.211	4.666	5.127

example is the L-shaped domain $\Omega := (-1, 1)^2 \setminus [0, 1] \times [-1, 0]$ with $\Gamma_D = \partial\Omega$ and the initial mesh \mathcal{T}_0 of Figure 6.3a. The piecewise constant volume force f reads

$$f(x, y) := \begin{cases} (0, -1) & \text{if } x \leq 0 \text{ and } y \geq 0, \\ (1, -1) & \text{if } x, y \geq 0, \\ (0, 0) & \text{if } x, y \leq 0. \end{cases}$$

Figure 6.5 displays the averaging and residual error estimators for a sequence of red-refined triangulations against the number of degrees of freedom. For $\mathbf{v} = 0.49, 0.499, 0.4999$ the values of the averaging error estimator lie on top of each other for all three FEMs, as well as the values of the residual error estimator. In Table 6.2 the quotients from (6.1) are approximated by the corresponding values of the averaging estimator. The values of these quotients are all of the same order of magnitude; this indicates no dependency on λ in the second inequality of (1.1).

Since f is a gradient, we do not expect and do not observe the locking behaviour while λ increases over several orders of magnitude.

6.5 L-shaped Domain with Neumann Boundary Conditions

This example confirms our theoretical findings in case of a non-empty Neumann boundary. The boundary conditions change type at the re-entering corner point. This causes the fact that one cannot expect a regularity of $H^{3/2+\varepsilon}$ for some positive ε . The empirical convergence rate $1/6$ of Figure 6.6 in terms of ndof clearly indicates that $u \notin H^{3/2}(\Omega; \mathbb{R}^2)$. This situation excludes even a mathematical justification via a straight-forward though technical generalisation of the error analysis from [KS95].

The domain Ω and the initial triangulation \mathcal{T}_0 is as in Subsection 6.4, while the volume force f reads

$$f(x, y) := \begin{cases} (0, 0) & \text{if } x \leq 0 \text{ und } y \geq 0, \\ (0, 1) & \text{if } x, y \geq 0, \\ (1, 0) & \text{if } x, y \leq 0. \end{cases}$$

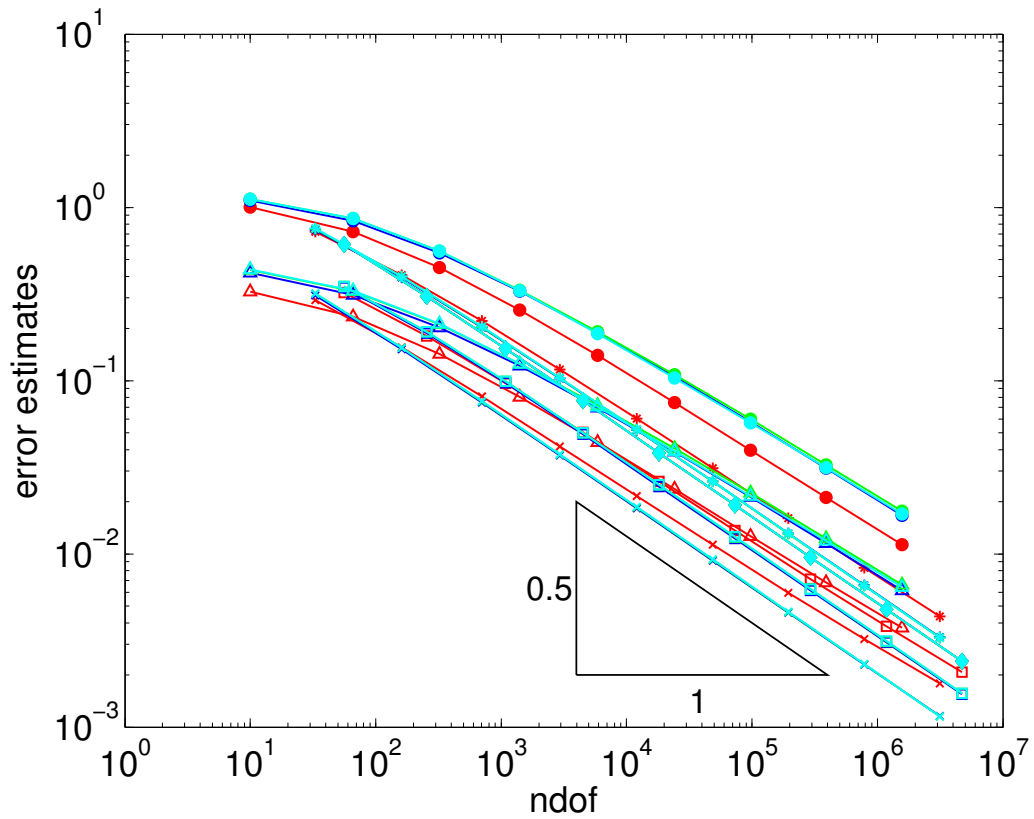


Figure 6.5: Estimated errors of CFEM (residual estimator (\bullet) and averaging estimator (\triangle)), CR-NCFEM (residual estimator (\blacklozenge) and averaging estimator (\square)), and KS-NCFEM (residual estimator ($*$) and averaging estimator (\times)) for $\nu = 0.4$ (red), 0.49 (blue), 0.499 (green), 0.4999 (cyan) on the L-shaped domain from Subsection 6.4.

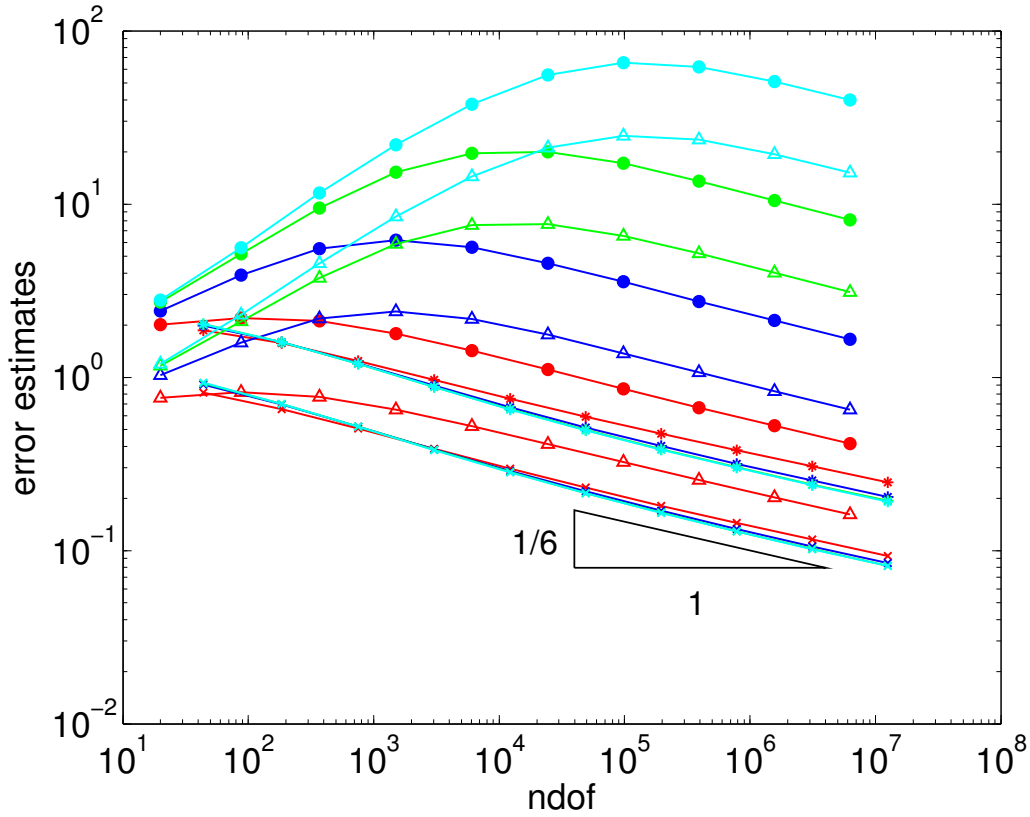


Figure 6.6: Estimated error for CFEM (residual estimator (\bullet) and averaging estimator (Δ)) and KS-NCFEM (residual estimator ($*$) and averaging estimator (\times)) for $\nu = 0.4$ (red), 0.49 (blue), 0.499 (green), 0.4999 (cyan) on the L-shaped domain from Subsection 6.5.

The boundary is divided in the Neumann boundary $\Gamma_N := \{(x_1, x_2) \in \partial\Omega \mid x_1 > 0\}$ with applied tractions $g \equiv 0$ and the Dirichlet boundary $\Gamma_D = \partial\Omega \setminus \Gamma_N$. Figure 6.6 displays the estimated errors in terms of the number of degrees of freedom. For $\nu = 0.499$ and 0.4999 , the values of the averaging error estimator for KS-NCFEM lie on top of each other, as well as the values of the residual error estimator for KS-NCFEM. The equivalence of KS-NCFEM and CFEM up to a multiplicative factor which scales linearly in λ is visible also for this singular problem. The numerical experiments provide striking empirical evidence for the robustness with respect to the locking behaviour and to possible singularities and mark the superiority of the somehow bizarre but simple and well-justified KS-NCFEM.

Acknowledgements

This work is supported by the DFG Research Center Matheon. The second author is also supported by the Berlin Mathematical School.

References

- [AF89] Douglas N. Arnold and Richard S. Falk. A uniformly accurate finite element method for the Reissner-Mindlin plate. *SIAM J. Numer. Anal.*, 26(6):1276–1290, 1989.
- [AW02] Douglas N. Arnold and Ragnar Winther. Mixed finite elements for elasticity. *Numer. Math.*, 92(3):401–419, 2002.
- [BB98] Weizhu Bao and John W. Barrett. A priori and a posteriori error bounds for a nonconforming linear finite element approximation of a non-Newtonian flow. *RAIRO Modél. Math. Anal. Numér.*, 32(7):843–858, 1998.
- [Bra07] Dietrich Braess. *Finite elements*. Cambridge University Press, Cambridge, third edition, 2007. Theory, fast solvers, and applications in elasticity theory, Translated from the German by Larry L. Schumaker, web supplements at http://homepage.ruhr-uni-bochum.de/Dietrich.Braess/FEM_corr_eng3.htm.
- [Bra09] Dietrich Braess. An a posteriori error estimate and a comparison theorem for the nonconforming P_1 element. *Calcolo*, 46(2):149–155, 2009.
- [Bre96] Susanne C. Brenner. Two-level additive Schwarz preconditioners for nonconforming finite element methods. *Math. Comp.*, 65(215):897–921, 1996.
- [Bre04] Susanne C. Brenner. Korn’s inequalities for piecewise H^1 vector fields. *Math. Comp.*, 73(247):1067–1087 (electronic), 2004.
- [BS92] Susanne C. Brenner and Li-Yeng Sung. Linear finite element methods for planar linear elasticity. *Math. Comp.*, 59(200):321–338, 1992.
- [BS08] Susanne C. Brenner and L. Ridgway Scott. *The mathematical theory of finite element methods*, volume 15 of *Texts in Applied Mathematics*. Springer, New York, third edition, 2008.

- [CEHL12] C. Carstensen, M. Eigel, R.H.W. Hoppe, and C. Löbhard. A review of unified a posteriori finite element error control. *Numerical Mathematics: Theory, Methods and Applications*, 5(4):509–558, 2012.
- [CF01a] Carsten Carstensen and Stefan A. Funken. Averaging technique for a posteriori error control in elasticity. III. Locking-free nonconforming FEM. *Comput. Methods Appl. Mech. Engrg.*, 191(8-10):861–877, 2001.
- [CF01b] Carsten Carstensen and Stefan A. Funken. A posteriori error control in low-order finite element discretisations of incompressible stationary flow problems. *Math. Comp.*, 70(236):1353–1381 (electronic), 2001.
- [CH] C. Carstensen and J. Hu. A linear nonconforming finite element method for the Stokes flow in three dimensional space. in preparation.
- [CPS12] C. Carstensen, D. Peterseim, and M. Schedensack. Comparison results of finite element methods for the Poisson model problem. *SIAM J. Numer. Anal.*, 50(6):2803–2823, 2012.
- [CR12] Carsten Carstensen and Hella Rabus. The adaptive nonconforming FEM for the pure displacement problem in linear elasticity is optimal and robust. *SIAM J. Numer. Anal.*, 50(3):1264–1283, 2012.
- [DDP95] Enzo Dari, Ricardo Durán, and Claudio Padra. Error estimators for nonconforming finite element approximations of the Stokes problem. *Math. Comp.*, 64(211):1017–1033, 1995.
- [Fal08] Richard S. Falk. *Finite Element Methods for Linear Elasticity*, volume 1939 of *Lecture Notes in Mathematics*. Springer-Verlag, Berlin, 2008. Lectures given at the C.I.M.E. Summer School held in Cetraro, June 26–July 1, 2006, Edited by Boffi and Lucia Gastaldi.
- [FM90] Richard S. Falk and Mary E. Morley. Equivalence of finite element methods for problems in elasticity. *SIAM J. Numer. Anal.*, 27(6):1486–1505, 1990.
- [Gud10] Thirupathi Gudi. A new error analysis for discontinuous finite element methods for linear elliptic problems. *Math. Comp.*, 79(272):2169–2189, 2010.
- [KS95] Reijo Kouhia and Rolf Stenberg. A linear nonconforming finite element method for nearly incompressible elasticity and Stokes flow. *Comput. Methods Appl. Mech. Engrg.*, 124(3):195–212, 1995.